Coordination Chemistry Reviews 509 (2024) 215817

Contents lists available at ScienceDirect

Coordination Chemistry Reviews

journal homepage: www.elsevier.com/locate/ccr

Redox-responsive inorganic fluorescent nanoprobes for serodiagnosis and bioimaging

Yuxin Liu [a,b,c,*], Zheng Wei [b], Francesco F. Mutti [b], Hong Zhang [b], Felix F. Loeffler [a,*]

[a] Department of Biomolecular System, Max-Planck Institute for Colloids and Interfaces, Potsdam 14476, Germany
[b] van' t Hoff Institute for Molecular Sciences, University of Amsterdam, Science Park 904, Amsterdam 1098 XH, The Netherlands
[c] Institute of Chemistry and Biochemistry, Free University of Berlin, Berlin 14195, Germany

ARTICLE INFO

Keywords:
Diagnostics
Nanomedicine
Therapy
Nanoparticles
Bioimaging

ABSTRACT

Redox reactions play fundamental roles in life and are at the core of metabolism. Thus, observing and quantifying these reactions is crucial for diagnostics and therapy. Recent advances in inorganic fluorescent nanoprobes have revolutionized the field, enabling *in vitro* diagnostics by providing reliable tools for real-time, quantitative determination of redox biomolecule levels in biological samples and cells. Due to their high stability, these probes are also widely used in bioimaging, providing real-time information for *in vivo* diagnostics and guiding treatment of diseases associated with redox biomolecules. This review explores the diverse landscape of inorganic fluorescent nanoprobes designed for the detection of biologically relevant reactive oxygen and nitrogen species. The discussion is divided into several sections, each focusing on nanoprobes tailored for specific oxidative species. The impact of tailored nanoprobes in diagnostics and imaging-guided treatment depends on their chemical composition, surface property, and fluorescence mechanism. The discussions highlight the current strengths and weaknesses, which will help to design more efficient redox-responsive inorganic fluorescent nanoprobes in the future.

1. Background

Biomolecules involved in reduction-oxidation (redox) reactions in living systems are essential for maintaining cellular homeostasis, metabolism, and signaling.[1,2] Based on their role in redox reactions, biomolecules are classified as oxidants and reductants. The best-known types of oxidants are reactive oxygen species (ROS)[3] and reactive nitrogen species (RNS)[4], which mainly include hydroxyl radicals (•OH), hypochlorite anions (ClO^-), hydrogen peroxide (H_2O_2), and peroxynitrites ($ONOO^-$). These ROS and RNS can damage biomacromolecules (*e.g.*, phospholipids, nucleic acids, and proteins), causing destruction, mutation, and dysfunction of cells.[5,6] In addition, they can activate inflammatory pathways within cells and generate inflammatory mediators that contribute to the occurrence of chronic inflammation.[7,8] As a result, the level of oxidants, such as ROS and RNS, can reflect changes in the redox state and thus be useful in the diagnosis of related diseases. Similarly, the concentration of reductants can also indicate the redox state as they are on the other side of the redox balance in living systems; that means, not only increased oxidant but also decreased reductant levels can be an indication of oxidative stress and, therefore, specific diseases.[9,10]. Typical reductive biomolecules are biothiols (*e.g.*, cysteine, homocysteine, and reduced glutathione),[11] reduced nicotinamide adenine dinucleotide (NADH) and its phosphate analogue (NADPH),[12] and flavin derivatives (*e.g.*, riboflavin, flavin adenine dinucleotide, and flavin mononucleotide),[13] which serve as oxidant scavengers or cofactors in various biological reactions.[14,15] Some exogenous reductants, such as ascorbic acid and polyphenols, can serve as biomarkers and are also widely used as drugs and dietary supplements.[16,17] In short, an abnormal change in redox biomolecule levels leads to pathological changes, such as occurrence and progression of inflammatory disorders,[18] diabetes,[19] cardiovascular diseases,[20] and neurodegenerative diseases.[21] Therefore, selective and accurate determination of redox biomolecule levels will enable diagnosis, guide treatment, and provide feedback for the management of related diseases.

Several methods have been proposed to identify these redox biomolecules. For different conditions and purposes, different detection methods are applied, ranging from chromatography,[22] colorimetry,[23] to electrochemical analysis[24], which are well known for their reliability, time resolution, and sensitivity, respectively. Compared to

* Corresponding authors.
E-mail addresses: yuxin.liu@mpikg.mpg.de (Y. Liu), felix.loeffler@mpikg.mpg.de (F.F. Loeffler).

https://doi.org/10.1016/j.ccr.2024.215817
Received 16 February 2024; Accepted 17 March 2024
Available online 21 March 2024

light absorption and electrochemical signals used in these methods, fluorescence imaging (fluorometry) is more suitable for diagnosis based on redox biomolecule detection because of its real-time capabilities, robustness in biological environments, high sensitivity, low background noise, and applicability to different biological scales (*e.g.*, organelles, cells, tissue slices, and living organisms). The above advantages make fluorometry feasible not only for *in vitro* serodiagnostics, but also for *in vivo* bioimaging, which is quite useful for diagnostics.[25,26] A rationally designed fluorescent probe can interact with one or more specific redox biomolecules, resulting in a change of fluorescence signals by wavelength, intensity, or lifetime.[27–29] Then, the level of redox biomolecule can be reflected by fluorescence signals in either collected biofluids or living organisms. On the one hand, the change of fluorescence signals can be easily recorded and analyzed by spectroscopy, while some of them (*e.g.*, wavelength and intensity) are even distinguishable to the naked eye.[30–32] This allows rapid evaluation of redox biomolecule levels at the point-of-care. On the other hand, benefiting from the development of charge-coupled devices and imaging technology, fluorescence bioimaging can perform high-resolution mapping and real-time tracking of specific redox biomolecules at the cellular level and *in vivo*, which contributes to continuous monitoring of pathological changes.[33–35] In short, by using appropriate probes, specific redox biomolecules can be identified and quantified by fluorimetry for both *in vitro* and *in vivo* diagnostics.

Traditionally, the fluorescent probes for the detection of redox biomolecules are organic molecular fluorophores, because most of them contain long conjugate chains that are active for oxidants.[36] Meanwhile, some functional groups, such as azides, are responsive to reductants.[37] Therefore, the detection of redox biomolecules is highly dependent on various organic reactions in the early stage of research. However, although these organic redox-responsive fluorescent probes can be selective and sensitive, there are many shortcomings. For example, most of them have broad fluorescence emission peaks that are unfavorable for the spectral multiplexing.[38,39] In addition, photobleaching limits their application in diagnostics due to reliability issues, especially in bioimaging.[40,41] There are more disadvantages of these organic probes and the details will not be discussed here, but stable fluorescent probes with narrow fluorescence peaks will be needed for the determination of redox biomolecules and the diagnosis of related diseases.

The first and most straightforward strategy is to replace the organic fluorescent core with more stable ones, such as fluorescent metal ions.[42–44] The redox biomolecules react with ligands of these inorganic molecular probes and affect the coordination field, thereby leading to fluorescence change. However, this type of probe still suffers from significant hydrophobicity issues. With the development of nanotechnology, the fluorescent metal ion-containing nanoprobes have received great attention, especially in the field of diagnostics.[45–47] Their fluorescence properties are modulable as organic fluorophores but much more stable in complex biological environments and upon repeated excitation. More importantly, due to electron shielding properties, their fluorescence emission peaks are narrow and well differentiated. As a result, these fluorescent metal ion-containing nanoprobes are welcomed for the determination of redox biomolecules and the diagnosis of related diseases. The redox biomolecules interact with the nanoprobes themselves or with ligands on their surface, and thereby triggering the fluorescence response through the inner filter effect (IFE)[48] and/or fluorescence resonance energy transfer (FRET) pathways.[49] Both pathways are accompanied by changes in the absorbance of the nanoprobes, but their mechanisms differ: While in IFE the fluorescence intensity changes through direct absorption of fluorescence, in FRET it changes through a non-radiative relaxation process caused by donor-to-acceptor energy transfer. It is worth mentioning that the detection mechanism of these nanoprobes is no longer limited by the organic reactions. Chemical changes induced by inorganic redox reactions and physical changes by non-covalent interactions can also affect the fluorescence of the nanoprobe.[50] Therefore, the use of these inorganic fluorescent metal ion-containing nanoprobes brings great opportunities to the diagnostic field by addressing the stability and hydrophilicity issues, while providing more flexibility. It also motivates further exploration of other redox-responsive inorganic fluorescent nanoprobes for diagnostics.

As delving deeper into the study of nanomaterials, some non-fluorescent inorganic materials are found to be fluorescent when their sizes is reduced to the Fermi wavelength, such as noble metals[51] and many semiconductor materials.[52] This unusual phenomenon contributes to the quantum confinement that occurs in all three dimensions of the ultrasmall dots, which leads to a discrete quantization of the energy levels of the electrons and the bandgap energy of the dot becomes size-dependent.[53–56] When these ultrasmall dots absorb photons, the electrons are excited. During the radiative relaxation, photons are released and fluorescence is emitted with the bandgap energy. The detailed mechanism and their differences are not discussed here, but as a result of the above theory, semiconductor quantum dots (QDs) and noble metal nanoclusters (NCs) are explored as new types of inorganic fluorescent nanoprobes.[57,58] According to the widely accepted terminology, most QDs are semiconductors (or carbon materials, which is beyond the scope of this review) with sizes between 2 and 15 nm, while NCs are generally metals or alloys with sizes below 2 nm (different from atomically precise clusters).[59] With appropriate functionalization, they can also be sensitive to the change of redox biomolecule concentration as fluorescent metal ion-containing nanoprobes. Due to the ultrahigh surface area, their fluorescence is more sensitive to the change of the surrounding environment, which is particularly useful for biodetection and serodiagnosis.[60,61] Notably, these redox-responsive inorganic fluorescent nanoprobes can also be used for the indirect determination of other biomolecules because the redox biomolecules are by-products of some biological reactions.[62,63] Therefore, they are not only useful for diagnostics of diseases related to redox biomolecules but to many substrate biomolecules in enzymatic reactions, which will be discussed in detail in the following sections.

Overall, the developed redox-responsive inorganic fluorescent nanoprobes have their own advantages in diagnostics, and their important role in this field is undoubtedly based on a considerable amount of experimental and industrial evidence. Given the advantages of fluorescent signals, these probes can be used not only for *in vitro* serodiagnostics, but also for *in vivo* bioimaging, enabling them to meet various diagnostic needs and provide real-time information to guide treatment (Fig. 1). This review focuses on how the impact of redox-responsive inorganic fluorescent nanoprobes in medical diagnostics basically depends on their chemical composition, surface property, and fluorescence mechanism. It aims to highlight the strengths and weaknesses of different inorganic fluorescent nanomaterials as redox-responsive nanoprobes. This will be useful to design more efficient redox-responsive inorganic fluorescent nanoprobes for diagnostics.

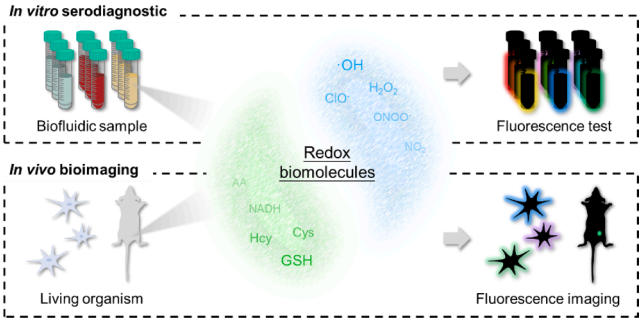

Fig. 1. Redox-responsive inorganic fluorescent nanoprobes for diagnostics through serodiagnostic and bioimaging pathways.

2. Oxidant-responsive nanoprobes

2.1. •OH-responsive nanoprobes

The •OH is one of the most reactive oxidants containing an unpaired electron, which makes it very capable of damaging cells and biomolecules in the body.[64] It is produced naturally as a byproduct of various biochemical reactions or by exposure to external sources, such as radiation and pollutants.[65] Excessively generated •OH will induce oxidative stress, which further leads to various diseases, including cancer,[66] diabetes,[67] cardiovascular diseases,[68] and neurodegenerative disorders.[69] Therefore, the •OH is a useful indicator not only for diagnosis but also for prevention of these diseases. However, due to its high reactivity, the •OH has a short lifetime ($\sim 10^{-9}$ s), thus being difficult to determine *in vitro*.[70] Therefore, most of the •OH-responsive inorganic fluorescent nanoprobes are designed for bioimaging *in vivo* (Table S1), which requires a relatively high signal-to-background ratio and deep tissue penetration.

In view of this, near-infrared (NIR)-excited lanthanide-doped nanoprobes are of interest. They are compatible and stable in various biofluids, and the NIR excitation generates low background fluorescence *in vivo*. In addition, the NIR excitation has much higher tissue penetration compared to traditionally used ultraviolet (UV) excitation. In 2015, Zhang *et al.* demonstrated the first example of a lanthanide-doped nanoprobe for ••OH quantification in solution.[71] The modified carminic acid received the energy from doped Er emitters and quenched their fluorescence at 510 nm by fluorescence resonance energy transfer (FRET). Since the carminic acid is easily decomposed by •OH, the fluorescence at 510 nm recovered in the presence of •OH. This work provided a good model for constructing an •OH-responsive lanthanide-doped nanoprobe; that is, modifying an •OH-responsive dye on an appropriate upconversion nanophosphor to quench its fluorescence. Very soon, Liu and his co-workers achieved •OH imaging and hepatitis diagnosis *in vivo* by using an azo dye-modified $NaYF_4$@$NaYF_4$:Yb, Tm@$NaYF_4$ nanoprobe.[72] The fluorescence of Tm emitters at 478 nm was quenched by the azo dye *via* FRET and recovered in response to •OH. The nanoprobe exhibited outstanding sensitivity with a limit of detection in the fM range, allowing sensitive •OH imaging in cells (Fig. 2A). As a further step, the nanoprobe was applied to a hepatitis mouse model, realizing fluorescence biopsy for hepatitis diagnosis (Fig. 2B). Following a similar thought, nanoprobes modified with other azo dyes[73] and phenothiazole dyes[74] are explored for the •OH imaging in cells and tissue sections. In addition, some works indicated that fluorescence ratiometry, including both working and reference fluorescence, can effectively improve the determination and diagnostic performance by reducing interference from samples.[75] However, with a deeper understanding of the FRET process, it was noticed that the reference fluorescence near to the working fluorescence was also affected by the modified dye as well, especially those emitted from higher energy levels than the working emission. This phenomenon decreased the change of fluorescence ratio per unit of •OH and thus the sensitivity of the nanoprobe. To minimize the influence of modified dyes on the reference fluorescence, Zhou *et al.* constructed Cypate-modified $NaErF_4$@$NaLuF_4$ as an •OH nanoprobe and used the short-wave infrared fluorescence of Er emitters at 1550 nm as a reference (Fig. 2C).[76] Compared with the traditionally used visible reference fluorescence in the visible range, at 540 nm, the one at 1550 nm was less influenced by the modified Cypate dye, which improved the sensitivity (0.00582 for 540 nm reference *vs.* 0.00912 for 1550 nm reference) around 2 times (Fig. 2D).

Apart from the performance of the developed nanoprobes, more attention has been paid in recent years to their practicality and sustainability. Since the oxidation of most organic dyes was irreversible, these dye-modified nanoprobes were disposable after •OH determination, resulting in a significant waste of resources. To address this issue, we constructed a recyclable lanthanide-doped nanoprobe based on 4-aminosalic acid (4-ASA)-Fe(II) complex.[77] After reaction with •OH, the 4-ASA-Fe(II) complex was oxidized to 4-ASA-Fe(III), which would generate absorbance by d-d transition and quench the fluorescence of Er at 540 nm. Notably, the Fe(III) in the complex could be easily reduced to Fe(II) by mild reducing agents (*e.g.*, ascorbic acid and reduced glutathione), resulting in the recovery of fluorescence without any obvious change in physical and chemical composition (Fig. 3A). Therefore, the designed nanoprobe could be recycled for at least 50 times (Fig. 3B). The diagnostic practicability for heavy metal-induced hepatoxicity was also demonstrated both at the cellular level and *in vivo* (Fig. 3C and D).

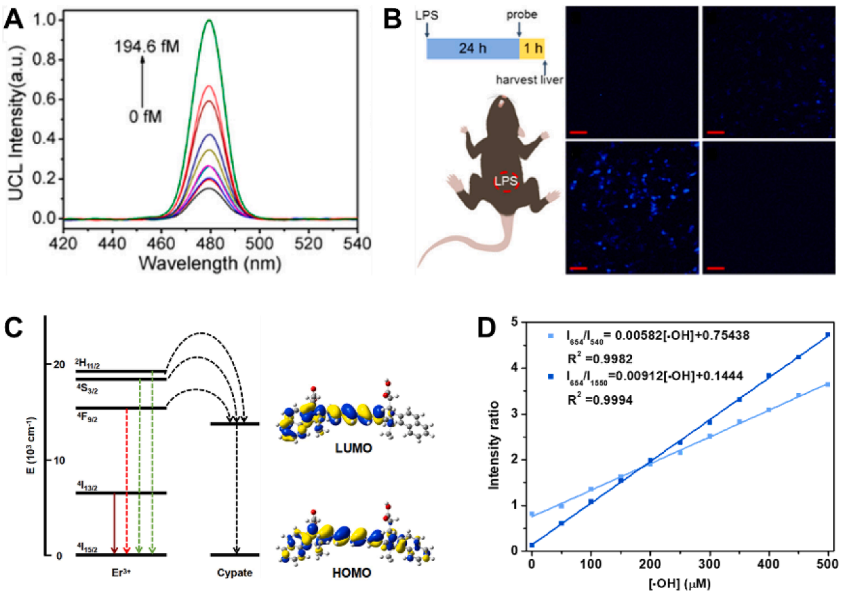

Fig. 2. (A) Emission of SWUCNPs (1.2 mg/mL) loaded with different concentrations of mOG. (B) Upconversion fluorescence imaging of mouse liver section. Mice were injected with lipopolysaccharides or physiological saline 24 h prior to nanoprobe injection. Images were acquired at 450–500 nm. Scale bar: 100 μm. Reproduced with permission.[72] Copyright 2015, American Chemical Society. (C) Proposed mechanism of energy transfer between csEr and Cypate, calculated by density functional theory. (D) Linear relationship between •OH concentrations and I_{654}/I_{540} and I_{654}/I_{1550} in the range from 0 to 500 μM. Reproduced with permission.[76] Copyright 2019, American Chemical Society.

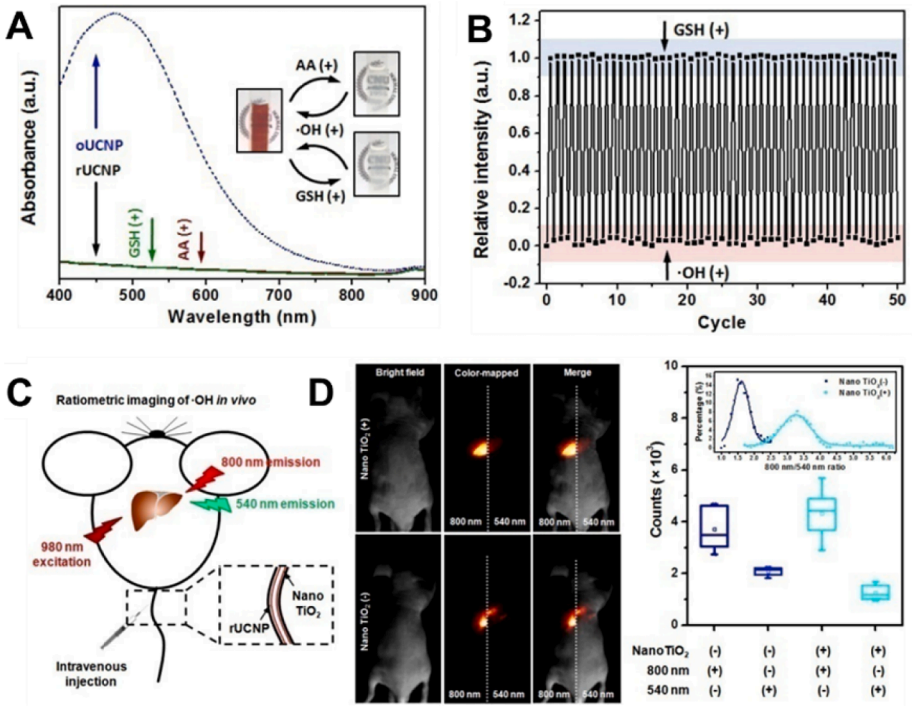

Fig. 3. (A) UV–vis-NIR spectra and photograph (insert) of rUCNP, oUCNP, and oUCNP treated with GSH and AA. (B) Monitoring 800 nm/540 nm of rUCNP recycled 50 times. (C) The diagram of •OH ratiometric imaging in vivo. (D) Bright-field, color-mapped luminescence, and merged images of mice with and without receiving nano TiO_2 injection. The box plot of luminescence intensity and 800 nm/540 nm ratio (insert) in the liver region from D. Reproduced with permission.[77] Copyright 2017, American Chemical Society.

In addition to the NIR-excited lanthanide-doped nanoprobes, QDs and NCs were also explored for •OH determination and diagnosis of related diseases, and possessed different •OH-responsive mechanisms. Lu *et al.* proposed a hole transfer mechanism to explain the fluorescence enhancement of CdTe QDs in •OH solution.[78] The •OH donates holes to the valence band of CdTe upon contact, which increases the density of excitons and the possibility of recombination. As a result, the fluorescence of CdTe QDs is gradually enhanced in response to an increasing concentration of •OH. Similarly, Wang *et al.* showed the fluorescence enhancement of Mn-doped Si QDs in the presence of •OH based on electron donation from radicals to the conduction band of the QDs.[79] In addition, the oxidation of QDs could also lead to so-called oxidation-induced quenching (OIQ) of the fluorescence. Zhou and co-workers found that the S-QDs were easily decomposed by •OH due to the oxidation and their fluorescence was quenched accordingly.[80] As for NCs, the aggregation-caused quenching (ACQ) effect was a widely used mechanism. Shao *et al.* demonstrated a ratiometric method for •OH detection by using denatured lysozyme-capped Ag NCs.[81] The denatured lysozyme was cross-linked by •OH and induced aggregation of Ag NCs, which mainly contributed to the fluorescence quenching. Meanwhile, the oxidation of Ag(0) in Ag NCs to Ag(I) by •OH was also found to be a potential reason for the fluorescence quenching. Like denatured lysozyme, oligonucleotides and thiols were also cross-linkable ligands by oxidation, which were also feasible for the detection of •OH.[82,83] These QDs- and NCs-based nanoprobes have also been applied to bioimaging. However, as their excitation wavelength was in the ultraviolet (UV) to blue light range, the penetration was limited and, therefore, only cell imaging was performed.

2.2. ClO^--responsive nanoprobes

Typically, the ClO^- is generated by myeloperoxidase-mediated peroxidation of chloride ions. Therefore, the elevated level of ClO^- is always associated with the abnormal activation of myeloperoxidase during severe infections and coronary artery disease. Therefore, it is also a valuable indicator for early diagnosis or classification of various diseases. Compared to the •OH, the ClO^- have longer lifetime in biofluidic samples, therefore, the nanoprobes would be useful for both *in vitro* serodiagnostics and *in vivo* bioimaging (Table S2).

Similar to the lanthanide-doped nanoprobes for •OH detection, the FRET mechanism was also a favorable mechanism for the construction of ClO^--responsive lanthanide-doped nanoprobes. Zhang *et al.* first demonstrated the feasibility of a rhodamine derivative-modified $NaYF_4$:Yb,Er,Tm nanoprobe for ClO^- detection. Subsequently, cyanine derivative,[84] metal complexes,[85,86] and MoS_2 nanosheets[87] were also utilized to construct ClO^--responsive lanthanide-doped nanoprobes. Following the same FRET mechanism, some QD-based nanoprobes were also constructed with Ag nanoparticles,[88] azobenzene derivative,[89] and curcumin[90] as energy acceptor. Utilizing these nanoprobes, imaging of ClO^- in various cells, zebrafish, and mouse was realized, while many disease models (*e.g.*, arthritis, inflammation, and hepatitis) were established and successfully diagnosed.

However, the traditional FRET-based nanoprobes are limited by the maximum fluorescence recovery; the energy acceptor quenches the fluorescence of the nanoprobe, so the possible maximum of fluorescence would be that of the original ones, which would reduce the response range for ClO^-detection. The traditional idea was to coat an inner or sensitizing layer on the lanthanide-doped nanoprobe to minimize surface defects and energy immigration to enhance the fluorescence, but the effect was quite limited.[91,92] In view of this, a dye-sensitized (DS) mechanism was introduced to the construction of ClO^--responsive lanthanide-doped nanoprobes. It was originally a practical strategy in solar cells to improve the light-harvesting efficiency. Here, the modified dye absorbs the excitation and then transfers the harvested photoenergy to the neighboring lanthanide ions (Fig. 4A). Therefore, the lanthanide ions are excited more effectively and the fluorescence is enhanced more significantly. Chen and co-workers reported IR808 dye-sensitized $NaGdF_4$:Yb,Er@$NaGdF_4$:Yb nanoprobe for HClO detection.[93] Under 808 nm laser irradiation, IR808 dye absorbed the photoenergy and then transfers it to Yb^{3+} and Er^{3+}, emitting strong green fluorescence

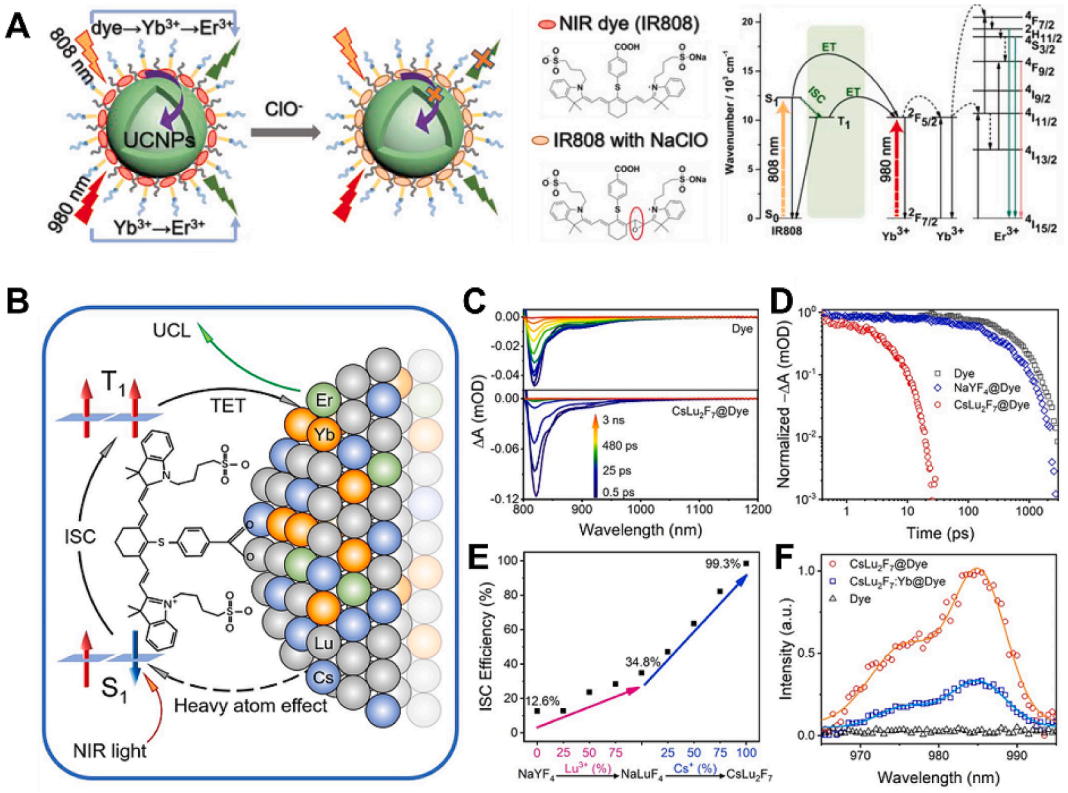

Fig. 4. (A) Schematic illustration of analyte-dependent energy transfer in NIR dye-sensitized upconversion nanoprobes, showing the composition of 980/808 nm dual-excitation nanoprobes and the mechanism of dye-sensitized upconversion fluorescence quenching by ClO^-. Energy transfer landscape, indicating intersystem crossing of NIR dye from the singlet (S1) to the triplet state (T1) before transfer to lanthanides. Reproduced under CC-BY 4.0 license.[93] (B) Schematic illustration of the intersystem crossing from S1 to T1 of IR808 due to the heavy atom effect of $CsLu_2F_7$:Yb/Er nanoprobes. (C) Femtosecond transient absorption spectra of free IR808 and IR808 in IR808-modified $CsLu_2F_7$ nanoprobes, respectively. The curve from blue to orange shows the stimulated emission at different delay times. (D) Kinetic curves of free IR808 and IR808 in IR808-modified $CsLu_2F_7$, $NaYF_4$ nanoprobes probed at the stimulated emission center (822 nm), respectively. (E) Intersystem crossing efficiency of the IR808 on the surface of a series of nanoprobes from $NaYF_4$ to $CsLu_2F_7$ with different concentrations of Lu^{3+} and Cs^+. (F) Time-resolved fluorescence spectra (delay time = 150 ms, gate time = 1 ms) of IR808-modified $CsLu_2F_7$ and $CsLu_2F_7$:Yb NCs upon excitation at 808 nm. Reproduced with permission.[94] Copyright 2022, Wiley-VCH.

centered at 541 nm. As Yb^{3+} cannot be directly excited by 808 nm irradiation, the 808 nm excited green fluorescence depends on the modified IR808 dye. When IR808 dye is decomposed by HClO, the green fluorescence excited by 808 nm is significantly quenched. At the same time, the 980 nm-excited green fluorescence, based on the direct absorption of Yb ions, is not affected by this change. Therefore, sensitive detection of ClO^- could be realized by using 808 nm-excited and 980 nm-excited green fluorescence as working fluorescence and reference fluorescence, respectively. After the successful implementation of the dye-sensitization strategy, the same group further proposed to enhance the fluorescence emission of the nanoprobes by using the heavy atom effect (Fig. 4B – F).[94] Similarly, Cy787,[95] IR 845,[96] and IR 792 dyes[97] were also applied to sensitize the lanthanide-doped nanoprobe for ClO^- detection, which combined both low detection limit and wide linear range.

However, although the dye-sensitization strategy improved the detection performance and benefited *in vitro* serodiagnosis, the working emissions were typically in the visible range, which would be unfavorable for bioimaging *in vivo* due to strong scattering. In view of this, Zhang *et al.* established a Cy7.5 dye-sensitized $NaYF_4$:Er@$NaYF_4$ nanoprobe, emitting fluorescence in the short-wave infrared (SWIR) range under either 808 nm or 980 nm irradiation (Fig. 5A).[98] Compared with the fluorescence in the visible and NIR range, the SWIR fluorescence can realize precise imaging of ClO^- *in vivo*, with a notable resolution of ~477 μm and penetration of 3.5 mm. Therefore, by using this nanoprobe, it is practical to diagnose lymphatic inflammation in mouse model by evaluating the concentration of generated ClO^- in lymph nodes. Subsequently, they also constructed glass scaffolds containing IR808 dye-sensitized $NaErF_4$@$NaYF_4$ nanoprobes, which were applied to provide accurate evaluation of angiogenesis and inflammation during bone repair (Fig. 5B and C).[99].

QDs were also applied for the detection of ClO^-, mainly *in vitro*, though based on different responsive mechanisms. Mancini *et al.* first reported the OIQ of CdSe-CdS-ZnS QDs in the presence of ClO^- due to the chemical oxidation of S and Se atoms on the surface.[100] This etching process increases the amount of lattice defects and results in the non-radiative relaxation. In addition, they also noticed that the polymer coating can reduce the etching effect, which provided a strategy to modulate the ClO^- responsive property of QDs. Huang and co-workers further studied the influence of polymer on the etching effect in detail.[101] QDs with a polymer protection bearing alkylamines or thiols showed lower sensitivity to ClO^- than those bearing $N(CH_3)_2$ groups, since functional groups can be reduced. Considering both sensitivity and cellular uptake, poly(maleic anhydride-alt-1-octadecene) was chosen to modify the QDs for ClO^- imaging in cells. These results guided the following construction of ZnO,[102] MoS_2,[103] and WSe_2 QDs[104] for OIQ-based ClO^- detection and imaging. Another interesting ClO^--responsive mechanism for QD nanoprobes is electron transfer from the conduction bands of Si QDs to electron-deficient ClO^-.[105].

Apart from the QDs, the metal NCs can also be oxidized and etched by ClO^-. Benefiting from their high surface area, the metal atoms on the NCs were highly active and thereby could be oxidized and ionized in the presence of ClO^-, generating defects and resulting in fluorescence quenching. Therefore, the Ag,[106] Cu,[107] Au,[108] and AuAg NCs

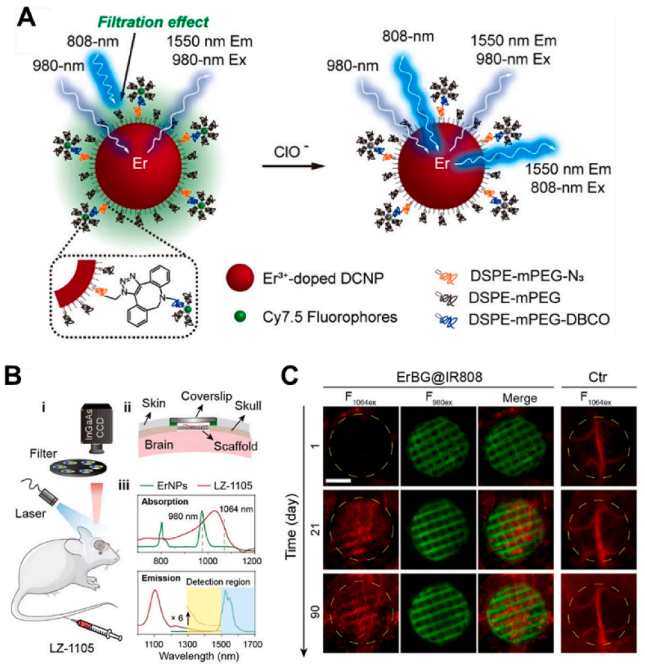

Fig. 5. (A) Schematic illustration of the ratiometric response of DCNP@Cy7.5 to HOCl based on an absorption competition-induced emission mechanism. When excitation is performed in the absorption overlapping region (808 nm), the fluorescence of DCNPs is quenched due to the energy filtration of excitation light by strongly absorbing Cy7.5. The quenching process is reversed after the degradation of Cy7.5 by HOCl oxidation. In the absorption non-overlapping region, the fluorescence of DCNPs under 980 nm excitation is unaffected, thus providing a ratiometric readout. Reproduced with permission.[98] Copyright 2019, American Chemical Society. (B) Schematic illustration of angiogenesis monitoring (i) and cranial window (ii), absorption and emission spectra (iii) of ErNPs and LZ-1105. (C) NIR-II fluorescence images of neovascularization in the bone defect region at different time points. Reproduced with permission.[99] Copyright 2022, American Chemical Society.

[109] were also explored as OIQ-based nanoprobes for ClO^- detection. Notably, the visible fluorescence of NCs can be captured by the naked eye and smartphone camera, which enables point-of-care and in-field detection of ClO^-. He and co-workers used a smartphone to record and analyse the fluorescence of QDs.[110] By taking photos of NC dispersions under daylight and 365 nm UV light, the ClO^- concentration could be semi-quantified according to the fluorescence intensity. However, most of the ClO^--responsive nanoprobes were based on oxidation, which made them suffere from •OH interference.

2.3. H_2O_2-responsive nanoprobes

H_2O_2 plays a vital role in most biological processes. It is not only a biomarker for diseases, but also an indicator of the concentration of other biomolecules and the activity of enzymes. Compared to •OH and ClO^-, many more inorganic fluorescent nanoprobes have been developed for H_2O_2 (Table S3). Most H_2O_2-responsive lanthanide-doped nanoprobes were based on the FRET and IFE mechanisms by using different dyes,[111–115] semiconductor nanomaterials,[116–118] and metal nanomaterials,[119] similar to the previously discussed •OH– and ClO^--responsive nanoprobes. Zhou and co-workers developed cyanine derivative-modified $NaYF_4$:Yb,Er,Tm nanoprobes for H_2O_2 imaging in inflammation models on cells, mice, and zebrafish.[111] The immune response induced by phorbol-12-myristate-13-acetate was monitored by using the H_2O_2-responsive ratiometric fluorescence of nanoprobes. To improve the tissue penetration and spatial resolution, Zhang *et al.* proposed an Er-sensitized $NaErF_4$:Ho@$NaYF_4$ nanoprobe with modification by the H_2O_2-responsive dye IR1061.[115] The nanoprobe was excited by 1530 nm irradiation and emitted two fluorescence bands in the NIR second window (NIR II) centered at 980 nm and 1180 nm, which can indicate the H_2O_2 concentration through oxidation of the IR 1061 dye. By doping the nanoprobe onto a microneedle patch, high-resolution detection of H_2O_2 and dynamic inflammation monitoring could be realized *in vivo* (200×200 μm). The QD- and NC-based nanoprobes were also constructed in a similar manner. For example, Dong *et al.* used Au nanoparticle-modified CdTe QDs to detect H_2O_2 through the IFE.[120] The $AuCl_4^-$ was reduced by H_2O_2, inducing the growth of Au nanoparticles and the increase of absorbance at 520 nm. Then, the fluorescence of CdTe QDs was quenched by competitive absorption. Nyokong *et al.* developed FRET-based nanoprobes based on the conjugation of CdTe-ZnS QDs to different H_2O_2-responsive metal tetraaminophthalocyanines and compared their difference on sensitivity and selectivity.[121] Chu *et al.* demonstrated tetramethyl benzidine (TMB)-modified Au NCs for H_2O_2 detection.[122] The Au NCs served as H_2O_2 catalysts, which induced oxidation of TMB and quenched the fluorescence of Au NCs. Compared to other energy acceptors, MnO_2 nanomaterials were the most widely used. Prasad *et al.* constructed MnO_2 nanosheets modified with $NaYF_4$:Yb,Er@$NaYF_4$:Yb,Nd nanoprobes for H_2O_2 detection.[123] The MnO_2 nanosheet could be decomposed by H_2O_2 and release Mn^{2+}, which resulted in fluorescence recovery (Fig. 6A). However, most remarkable in this approach is the ability of the released Mn ions to act as a catalyst for the decomposition of hydrogen peroxide.

2.3.1. H_2O_2-responsive imaging-guided tumor treatment

Due to the limited oxygen delivery and rapid metabolism, the intratumoral H_2O_2 level is elevated, which has been explored as a potential target for tumor treatment.[124] In tumors, the MnO_2 decomposes, which not only allows fluorescence imaging for tumor diagnosis, but it can also catalyze the decomposition of endogenous H_2O_2, generating oxygen, alleviating the intratumoral hypoxia, and sensitizing it to oxygen-dependent tumor treatment. Shi *et al.* used MnO_2 nanosheet-modified $NaYF_4$:Yb,Er,Tm nanoprobes to improve the intratumoral oxygen content and enhance radiotherapy (Fig. 6B).[125] Zhang and Xing reported MnO_2 nanosheet-modified $NaYF_4$:Yb,Tm@$NaYF_4$ and MnO_2 nanosheet-modified $NaYF_4$:Yb,Tm,Nd@$NaYF_4$:Nd nanoprobes to sensitize the tumor for photodynamic therapy.[126,127] In addition, utilizing the paramagnetism of Mn^{2+}, Lin *et al.* further demonstrated a mesoporous MnO_2-coated $NaGdF_4$:Yb,Er nanoprobe for H_2O_2-activated T_1-weighted magnetic resonance imaging (MRI) to provide information with high spatial resolution, which was complementary to fluorescence imaging with high temporal resolution.[128] Therefore, the use of MnO_2 as an energy acceptor allows the expansion from tumor diagnostics to therapy. Similarly, QDs[129–132] and NCs[133,134] were also functionalized with MnO_2 nanomaterials as FRET-based H_2O_2 nanoprobes for *in vitro* detection and *in vivo* imaging. For example, Sun *et al.* showed MnO_2 nanosheet-modified Ag_2Se QDs for the NIR II fluorescence imaging of H_2O_2 and production of oxygen inside the tumor for radiotherapy sensitization (Fig. 6C – F).[131] Therefore, with a rationally designed chemical composition, H_2O_2-responsive fluorescent nanoprobes are feasible for tumor imaging-guided treatments that use elevated intratumoral H_2O_2 levels as a target.

2.3.2. Enzyme-based detection of other biomolecules

Beside tumor treatment, another important application for these H_2O_2-responsive fluorescent nanoprobes is the detection of other biomolecules based on enzymatic reactions (Table S4). Among all the different reactions, glucose oxidase-catalyzed oxidation of glucose is the most studied. On the one hand, glucose is the essential indicator to evaluate the onset and progression of diabetes, one of the most dangerous metabolic diseases of the last decades. On the other hand, this reaction is thoroughly studied and therefore a typical model for enzyme-based biodetection. Chu *et al.* utilized MnO_2 nanosheet-modified $NaYF_4$:Yb,Tm@$NaYF_4$ for the detection of glucose in blood using glucose

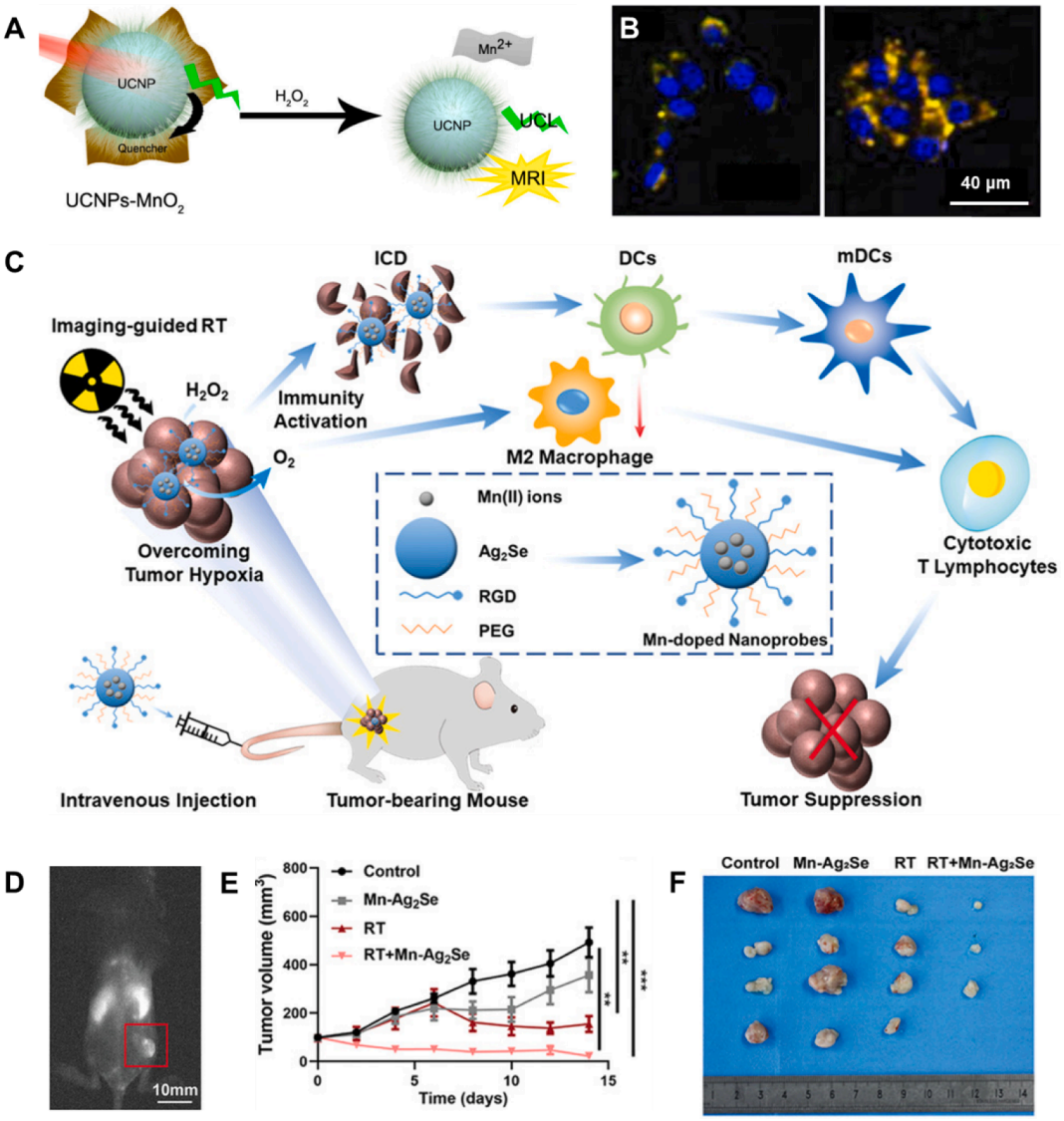

Fig. 6. (A) Schematic diagram of H_2O_2-responsive UCNPs-MnO_2. Reproduced with permission.[123] Copyright 2018, American Chemical Society. (B) Confocal laser scanning microscopy images of hc-4 T1 cells after incubation with UCSMs for 8 h (left) and 20 h (right), respectively. The nucleus is stained with DAPI to emit blue luminescence while the UCNP core of UCSMs could emit yellow luminescence (merging of green and red luminescence) upon NIR excitation. Reproduced with permission.[125] Copyright 2015, Wiley-VCH. (C) Schematic illustration of oxygen self-supply nanoprobe emitting in the NIR-II window to guide and enhance radiotherapy by promoting anti-tumor immunity. (D) Fluorescence imaging of mice after intravenous injection of Mn-doped nanoprobes at time intervals of 24 h. (E) Tumor volume growth curves of different groups of mice during 14 days after various treatments. (F) Photos of excised tumors from mice on day 14 after different treatments. Reproduced with permission.[131] Copyright 2021, Wiley-VCH.

oxidase (GOx).[135] This nanoprobe possessed a low detection limit of 3.7 μM in buffer and can vary in blood samples. However, as the MnO_2 can also be degraded by biothiols, which will be discussed later, this nanoprobe would be significantly affected by the high concentrations of GSH and cysteine in biofluids. Therefore, better energy acceptors were developed for glucose-responsive lanthanide-doped nanoprobes, such as Ag nanoparticles,[136] Au nanoparticles,[137] a squaric acid-Fe(III) complex,[138] and dopamine.[139] These energy acceptors provided better selectivity to the nanoprobes as they were not sensitive to biothiols. In addition, the joint use of multiple enzymes can also improve the selectivity.[140,141] Wang *et al.* reported the combination of GOx, horseradish peroxidase (HRP), TMB, and $NaYF_4$:Yb,Er for the detection of glucose.[140] The GOx catalyzed the oxidation of glucose to produce H_2O_2 as a byproduct, which can oxidize TMB through a HRP-catalyzed reaction. Since the TMB was inert to most biomolecules, the enzymatic cascade reaction is orthogonal to the cell metabolism due to the high selectivity of GOx and the reactivity of TMB in presence of HRP. Rhee *et al.* used the same cascade reaction and CdSe-ZnS QDs for glucose detection.[142] The HRP-induced H_2O_2 decomposition directly resulted in the oxidation of the QDs, forming the oxidation defects and quenching the fluorescence. Su *et al.* further utilized Fe_3O_4 to replace HRP in this cascade reaction and realized much more sensitive glucose detection.[143] Following a similar thought, H_2O_2-responsive nanoprobes have also been developed for the detection of alcohol,[144] uric acid,[145,146] lactate,[147,148] choline,[149,150] acetylcholine,[134,149,151] and xanthine[152] by using corresponding enzymes. Notably, recent works paid more attention on the sustainability and construction of devices. For example, Willner *et al.* presented DNA-stabilized Ag NCs as a reversible H_2O_2 nanoprobe.[153] In the presence of H_2O_2, oxidative traps formed on the surface and the fluorescence of Ag NCs was quenched, but this oxidation process could be reversed by using ascorbic acid. However, due to material limitations, the fluorescence of Ag NCs could be quenched by quinones, resulting in a reduced selectivity. In addition, Koh *et al.* constructed a microfluidic bioassay

based on hydrogel entrapping glucose oxidase and alcohol oxidase-conjugated QDs (Fig. 7).[144] The hydrogel arrays were prepared by photolithography in the microchannels, generating multi-color patterns for simultaneous detection of glucose and alcohol.

2.4. Onoo⁻-responsive nanoprobes

$ONOO^-$, one of the most typical RNS, is also associated with many different diseases, especially chemical liver injury, for example, the apoptotic hepatocytes will activate the Kupffer cells in response to overdose of paracetamol and trigger the generation of RNS. In contrast to •OH, the oxidative property of $ONOO^-$ is more selective to specific organic structures and functional groups. Therefore, more attention has been paid to the design and construction of $ONOO^-$-responsive molecules, and thus most inorganic fluorescent nanoprobes for $ONOO^-$ detection are conjugated with organic dyes based on the FRET mechanism (Table S5). Peng *et al.* designed a $ONOO^-$-responsive cyanine derivative and conjugated it with $NaYF_4$:Yb,Tm@$NaYF_4$ nanoparticles.[154] The fluorescence intensity of the nanoprobe was positively dependent on the $ONOO^-$ concentration, which would be useful to indicate paracetamol-induced hepatotoxicity. With a similar thought, the same group developed many different $ONOO^-$-responsive dyes for functionalization of lanthanide-doped nanoparticles to improve selectivity and sensitivity, such as pyran,[155] quinoneimine,[156] and other cyanine derivatives.[157].

In addition, Wang *et al.* tuned the working and reference emission to the NIR II wavelength range to improve tissue penetration for *in vivo* $ONOO^-$ imaging.[158] By constructing an A1094 dye-conjugated $NaErF_4$@$NaYF_4$@$NaYF_4$:Nd@$NaYF_4$, the two NIR II fluorescence emissions centered at 1060 nm, the $ONOO^-$-responsive working emission, and 1550 nm, the reference emission, were combined for ratiometric imaging and diagnosis of hepatotoxicity in a mouse model. To simplify the chemical structure of the nanoprobe, they utilized QDs to replace the complex core-multi-shell lanthanide-doped nanoparticles as the fluorescence donor. By using the same A1094 dye as the fluorescence acceptor, a Ag_2S QDs-based nanoprobe was constructed to study the generation of $ONOO^-$ in traumatic brain injury (Fig. 8).[159] Instead of studying the structure of the nanoprobe, Wang and co-workers paid more attention to expanding the application scenario of these $ONOO^-$-responsive nanoprobes, including ischemic stroke,[160] acute myeloid leukemia,[161] and peripheral vascular disease.[162].

2.5. Inorganic fluorescent nanoprobes for other biological oxidants

In addition to those specifically introduced above, inorganic fluorescent nanoprobes that respond to other biological oxidants are also available, but only limited work exists. For example, Han *et al.* demonstrated the application of Au NCs for cell imaging of superoxide anion radicals ($\bullet O_2^-$), which was realized by the fluorescence quenching effect of $\bullet O_2^-$ due to the oxidation of Au atoms in NCs.[163] Wang *et al.* reported a carbon nanodot-functionalized CdTe QDs for visual detection of NO_2 with a low limit of detection of ~19 nM, which would be useful for point-of-care serodiagnosis of NO_2-related diseases.[164].

3. Reductant-responsive nanoprobes

3.1. Biothiol-responsive nanoprobes

Biothiols are a class of biomolecules that contain sulfhydryl groups, which play a vital role in regulating cellular redox balance, maintaining the tertiary structure of proteins, and in detoxification processes. Among them, three have attracted the most attention due to their characteristic functions, namely cysteine (Cys), homocysteine (Hcy), and reduced glutathione (GSH). Therefore, most of the biothiol-responsive nanoprobes were designed trageting these three biomolecules.

3.1.1. Cys/Hcy-responsive nanoprobes

Cys is an amino acid necessary for cell regeneration, while Hcy, with only one additional methylene group in its chemical structure, is an experimental indicator of cardiovascular diseases such as coronary artery disease and pulmonary embolism. The design of both Cys- and Hcy-responsive nanoprobes always focuses on their sulfhydryl, which is a strong reducing functional group (Table S6). Li *et al.* constructed yolk-shell $NaLuF_4$:Yb,Er,Tm nanoparticles to encapsulate Cys/Hcy recognition dyes for the construction of a FRET-based nanoprobe.[165] Compared with other structures, this yolk-shell nanoparticle can afford more dyes in its hollow interior, thus showing excellent FRET efficiency. Although it cannot identify Cys and Hcy well, Cys imaging in cells was still realized as the concentration of Hcy in normal cells is quite low. Afterwards, some similar FRET-based nanoprobes were presented, based on lanthanide-doped nanoparticles, but the selectivity did not improve.[166,167] Similarly, QDs were used for Cys/Hcy detection based on the FRET mechanism.[168] Not surprisingly, the mechanism becomes different when it comes to NCs. Shang and Dong studied the fluorescence of Ag NCs in the presence of Cys and proposed the mechanism of the fluorescence quenching effect.[169] The Ag atoms on the surface of the NCs formed Ag-S bonds with Cys and became reactive, which made them much easier to be oxidized by the dissolved oxygen in water, thereby inducing the fluorescence quenching. Since the concentration of Cys in biofluids is significantly higher than that of Hcy, up to date, there are no reliable inorganic fluorescent nanoprobes that can identify Hcy without any influence from Cys in biofluids.

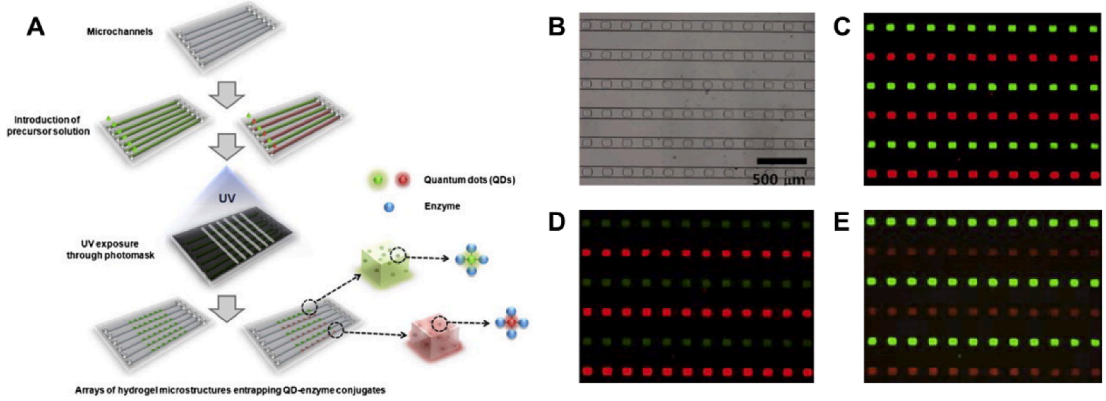

Fig. 7. (A) Schematic illustration of fabricating arrays of hydrogel microstructures entrapping QD-enzyme conjugates in microfluidic devices. (B) Light-field and (C) fluorescence image of six microchannels incorporating hydrogel microarrays entrapping QD-GOx (green) and QD-AOx conjugates (red). Fluorescence images obtained after filling the microchannels with (D) glucose only solution or (E) alcohol only. Reproduced with permission.[144] Copyright 2012, Elsevier Ltd.

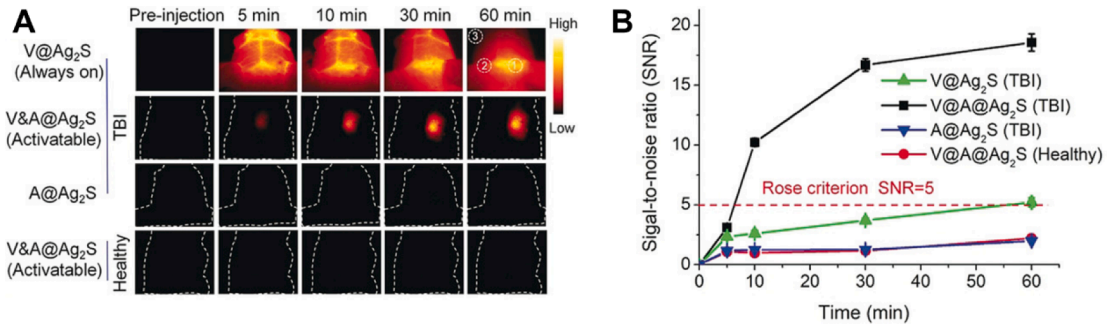

Fig. 8. (A) Time course of NIR-II fluorescence in mice with vascular brain injury and healthy mice at different time points after injection of V@Ag_2S, V&A@Ag_2S, and A@Ag_2S. (B)Time-dependent signal-to-noise ratio changes determined by the NIR-II fluorescence imaging of mice after different treatments. Reproduced with permission.[159] Copyright 2020, Wiley-VCH.

3.1.2. *GSH-responsive nanoprobes*

GSH is a tripeptide biothiol consisting of cysteine, glutamic acid, and glycine. It is abundant in living organisms and plays a vital role in detoxification, maintaining cellular redox balance, and protecting cells from oxidative stress.

Deng and co-workers reported the MnO_2 nanosheet-modified $NaYF_4$:Yb,Tm nanoprobe for imaging of GSH in cells.[170] Like those MnO_2-modified nanoprobes with H_2O_2 responsive property, the MnO_2 nanosheet was decomposed by GSH, which resulted in fluorescence recovery and can show the GSH distribution in cells. Based on a similar FRET strategy, many GSH-responsive nanoprobes were constructed by using lanthanide-doped nanoprobes[171–173] and QDs.[174–176] When it came to NCs, the GSH-responsive mechanism was different. Chen *et al.* observed that the in the presence of GSH, the fluorescence of histidine-capped Au NCs was significantly and linearly enhanced. To explain this phenomenon, they proposed that the GSH replaces the histidine cap on the surface of Au NCs through the formation of Au-S bonds, and then donates electrons to the Au NCs, which not only minimizes the surface quenching effect but also increases the probability of radiative recombination.[177] Following this mechanism, Au NCs with other capping were also explored as nanoprobes for GSH detection and imaging.[178,179] Further efforts have been made to bioimage GSH *in vivo*. To improve the sensitivity of the nanoprobe to the intratumoral GSH level, Liu *et al.* proposed a Cy-GSH dye-modified $NaYF_4$:Yb,Er@$NaYF_4$:Nd nanoprobe based on dye-sensitization strategy, which achieved a significantly improved signal-to-background ratio of ~30 (Fig. 9A and

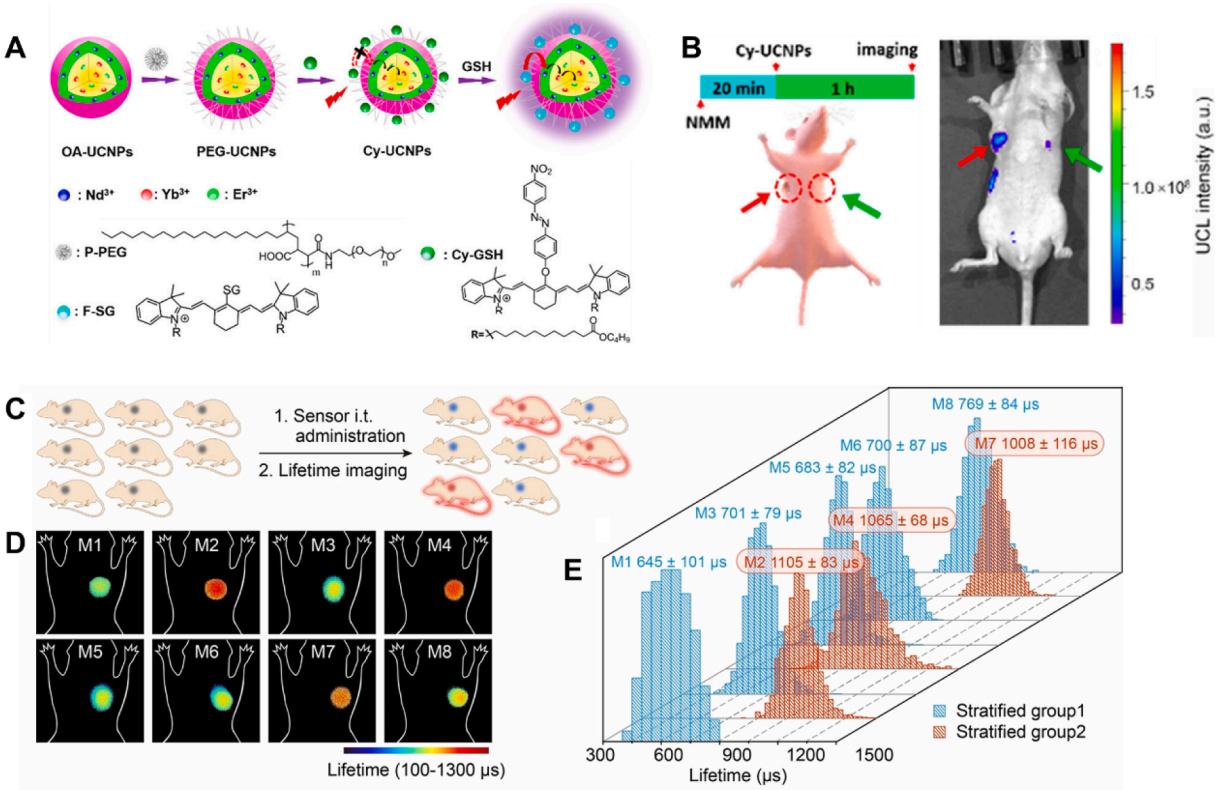

Fig. 9. (A) Schematic illustration of the construction of Cy-UCNPs probes and the detection of GSH by target-modulated sensitization. (B) In vivo upconversion fluorescence images after injection of 50 μL Cy-UCNPs (20 mg kg^{-1} body weight) for 1 h in tumor tissues (red arrows) and opposite normal tissues (green arrows). The mice were preintravenously injected with 50 μL saline (a) or 50 μL N-methylmaleimide (20 mg kg^{-1} body weight) (b) 20 min before Cy-UCNPs injection. Reproduced with permission.[180] Copyright 2018, American Chemical Society. (C)Schematic illustration of the blinded study of eight tumor-bearing mice. (D)NIR-II luminescence lifetime images of tumor bearing mice. (E)Luminescence lifetime distribution of the eight tumors. Reproduced with permission.[182] Copyright 2022, Wiley-VCH.

B).[180].

3.1.3. GSH-responsive tumor treatment

Notably, GSH levels in blood and major organs are relatively high (25 – 1000 μM), and are significantly elevated in malignant tumors (>3000 μM) due to intratumoral hypoxemia and inflammation. Therefore, GSH-responsive nanoprobes are more likely to be used in selective imaging of tumors and guidance of therapy (Table S7). Lin *et al.* reported a Pt(IV) complex-functionalized $NaYF_4$:Yb,Tm nanoprobe for GSH-responsive bioimaging and chemotherapy of tumors.[181] The ultraviolet and blue emissions of Tm were quenched by Pt(IV) complex, and recovered in the presence of GSH as the Pt(IV) complex was reduced to cisplatin. The produced cisplatin was a typical chemo-drug that will induce apoptosis of tumor cells, thereby realizing fluorescence imaging-guided chemotherapy *in vivo*. As the unavoidable and inhomogeneous signal intensity attenuation hampers the quantification of GSH concentration, the fluorescence intensity always leads to false results in deep tissue. In view of this, Chen *et al.* demonstrated a series of lanthanide-doped nanoprobes for the quantification of GSH *in vivo*.[182] The energy transfer to MnO_x reduced the fluorescence lifetime of the lanthanide-doped nanoprobe, and was blocked when MnO_x was reductively decomposed by GSH. Therefore, in the presence of GSH, the lifetime of MnO_x-modified lanthanide-doped nanoprobes increased and was linearly related to the GSH concentration. The lifetime was an intrinsic property of the nanoprobe that was not affected by the absorbance and scattering of biosamples and thereby allowed quantitative analysis in deep tissues (Fig. 9C and D). By analyzing the fluorescence lifetime of nanoprobes in tumors, the intratumoral redox state can be detected non-invasively in real-time, which has been used for subsequent therapeutic guidance for precise tumor treatment (Fig. 9E).

Although intratumoral GSH can be quantified through imaging and is available to guide tumor treatment, the previous works neglected the individual differences in intratumoral conditions, which are quite common in the solid tumor cases due to their unpredictable intratumoral oxidative stress. It leads to unpredictable therapeutic performance. Consequently, we proposed a customized photothermal therapeutic mode to meet individual treatment demands.[183] The intratumoral GSH levels were individually determined by fluorescence imaging and linked to the GSH-dependent photothermal conversion property of the nanoprobe. To guide the treatment, we constructed nine tumor models with different redox states and nanoprobe accumulations and measured temperature changes under different laser prescriptions as a reference (Fig. 10A). Based on these results, an individual laser prescription, including laser power density and irradiation time, is determined for

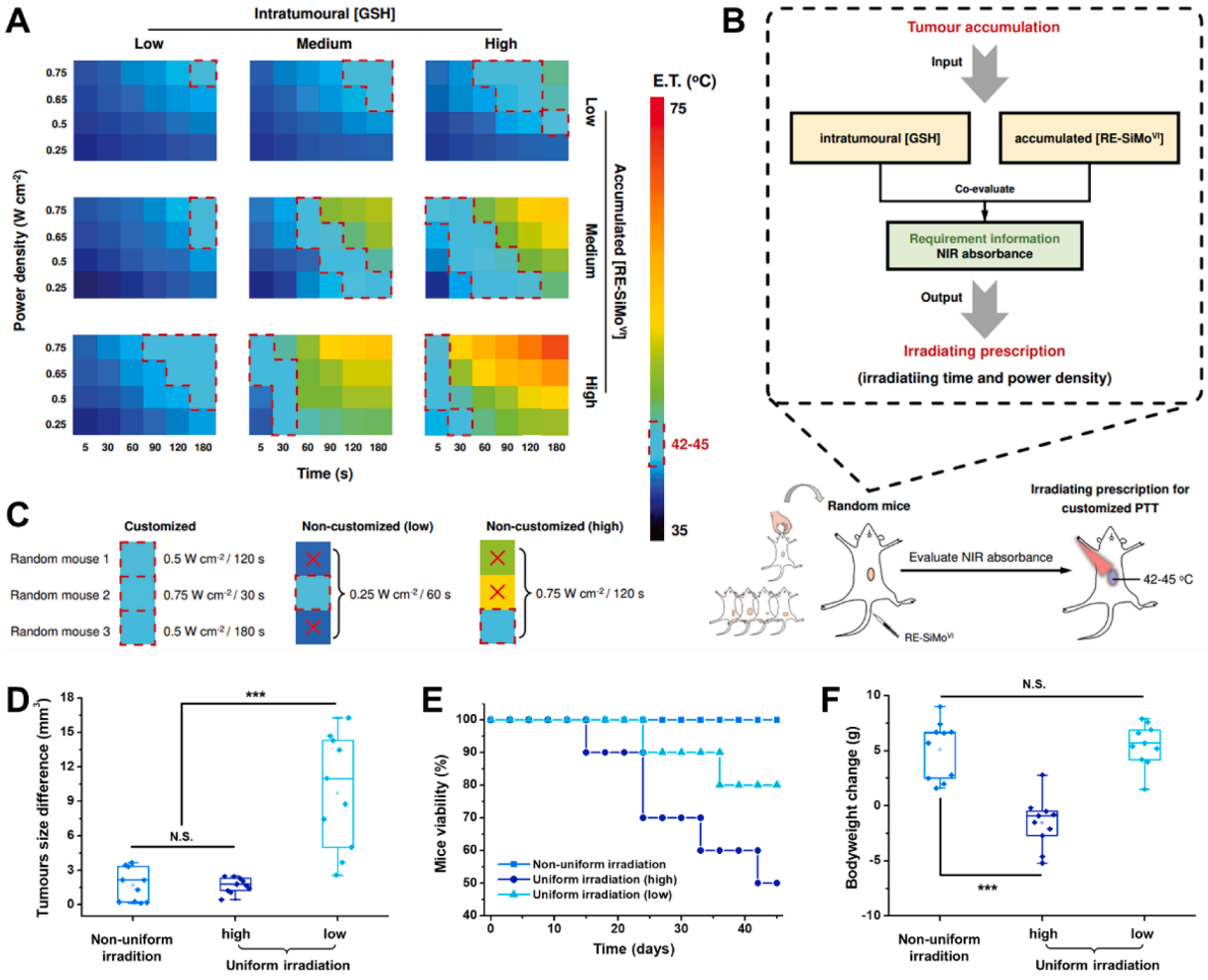

Fig. 10. (A) The Eigen temperature (E.T.) of rRE-SiMo under different irradiation power density and time in vivo. The rRE-SiMo was formed in situ in nine typical intratumoral conditions with two variable factors including intratumoral (GSH) and accumulated (RE-$SiMo^{VI}$). (B) Scheme of optimization of irradiation prescription (irradiation power density and time) for customized photothermal therapy of randomly selected mice. (C) The E.T. of rRE-SiMo in three randomly selected mice after receiving customized irradiation and unified high or low irradiation prescriptions (non-customized). The E.T. in the effective range (42–45 °C) is outlined by a dark-red dotted line. The E.T. outside the effective range is marked by a red cross. Reproduced with permission.[183] Copyright 2021, Wiley-VCH. Difference in (D) tumor size, (E) viability, and (F) body weight change of mice after 12 days receiving non-uniform irradiation according to the customized prescription (n = 10). Mice receiving uniform high and low irradiation were used for comparison. Reproduced with permission.[184] Copyright 2023, Wiley-VCH.

each case to raise the temperature to a safe range for therapy (42–45 °C); that is, a stronger laser and longer irradiation time were used for the cases with lower intratumoral GSH levels, while weaker and shorter irradiations were used for the higher cases (Fig. 10B and C). Thus, all cases received effective photothermal treatment with less risk of over-treatment. In a further step, we expanded the customized therapeutic strategy to the GSH difference between multiple tumors in the same individual.[184] Customized laser prescriptions were established for each tumor and performed by using a self-constructed laser array. By utilizing the synergistic effect of photothermal therapy and chemotherapy, simultaneous and efficient treatment of multi-tumor cases was successfully achieved (Fig. 10D – F).

Due to their characteristic sulfhydryl group, biothiols could be distinguished from other biological reductants. However, it is still difficult to selectively identify individual biothiols because all of their reducing properties contribute to the sulfhydryl group, which would be unfavorable for biodetection and precise diagnosis.[185–188].

3.2. Ascorbate-responsive nanoprobes

Unlike biothiols, ascorbates are not endogenous biological reductants in the human body due to lack of L-gulonolactone oxidase. However, it is involved in many biological processes (*e.g.*, biosynthesis of norepinephrine as a cofactor of dopamine β-hydroxylase) and is associated with various diseases (*e.g.*, scurvy). Therefore, it is widely used in dietary supplements, whereas ascorbate-responsive nanoprobes can indicate disease progression and evaluate health status (Table S8).

Sakka *et al.* reported a $CePO_4$:Tb nanoprobe for the determination of ascorbate.[189] In the presence of $KMnO_4$, the Ce^{3+} in the nanoprobe is oxidized to Ce^{4+}, resulting in the reduction of energy transfer from Ce^{3+} to Tb^{3+} under UV excitation. Similarly, Yan *et al.* demonstrated $KMnO_4$-treated CdTe QDs as ascorbate nanoprobes by using the reversible Te^{2-}-Te^{4+} cycle.[190] Therefore, the fluorescence was quenched and can be recovered by adding reducing agents, such as ascorbates. Then, Chu *et al.* constructed a FRET-based nanoprobe for ascorbate determination by using CoOOH nanosheet as an energy acceptor, which is quite similar to their MnO_2-functionalized H_2O_2-responsive nanoprobe.[191] By a similar thought, Au NCs with L-DOTA-Fe(III) complex and MnO_2 as energy acceptor were also established by Sony's and Wang's groups.[192,193] Apart from the above two mechanisms, Liang *et al.* demonstrated an unusual dye-sensitization method to selectively detect ascorbate over other reductants. They prepared a CyBSO-sensitized $NaYF_4$:Yb,Er nanoprobe and found that its fluorescence can be enhanced by triethylamine because it increases the nucleophilicity of the solvent and leads to dye shedding from the nanoparticles. However, ascorbate can react with triethylamine and eliminate this effect, thereby quenching the dye-sensitized fluorescence. Since other biological reductants, such as the studied Cys, did not react with triethylamine, this nanoprobe showed extraordinary selectivity for ascorbate.[194] Another interesting approach was made by Nie and co-workers by realizing imaging of ascorbate in cells and living animals.[195] They constructed a dual-emitting Au NCs-PbS QD nanocomposite as the ascorbate-responsive nanoprobe. The fluorescence of PbS QDs at 813 nm is quenched by ascorbate due to electron transfer, while the fluorescence of Au NCs at 640 nm remained stable, which enabled the ratiometric imaging of ascorbate *in vivo*.

Notably, like the H_2O_2-responsive nanoprobes, the ascorbate-responsive nanoprobes can also be used to evaluate enzymatic activity. Jin *et al.* noticed that alkaline phosphatase can induce the hydrolysis of L-ascorbic acid 2-phosphate and produce ascorbate.[196] Therefore, the activity of alkaline phosphatase, which is a clinical indicator of liver injury, can be determined using ascorbate-responsive CdSe-ZnS@Au hybrid nanoprobes. By tracking the change in the fluorescence signal, the activity of alkaline phosphatase can also be monitored by fluorescence imaging in cells.

3.3. Inorganic fluorescent nanoprobes for other biological reductants

In addition to biothiols, NAD(P)H and flavin derivatives are important endogenous biological reductants. Since they always act as co-factors in enzymes, the determination of NADH and flavin derivatives is also useful to evaluate the enzymatic activity. Willner and co-workers applied Nile Blue-functionalized CdSe-ZnS to determine NADH levels in the NAD^+-dependent biotransformation process of alcohol dehydrogenase and D-glucose.[197] It can monitor the biocatalytic reaction *in vitro* as well as the intracellular metabolic pathway through fluorescence imaging. As for the flavin derivatives, due to their conjugated structure, they have strong absorbance in the blue spectral region and are themselves energy acceptors for fluorescence detection. For example, Natrajan *et al.* used the blue emission of Gd_4O_2S:Yb,Tm at 475 nm to detect flavin mononucleotide (FMN) by FRET.[198] Since the reduced form of FMN is colorless, this nanoprobe can also report the turnover of flavoproteins (*e.g.*, pentaerythritol tetranitrate reductase). Interestingly, the same group used a similar strategy to achieve fluorescence detection of NADPH that uses flavoenzyme pentaerythritol tetranitrate reductase as the energy acceptor of the Gd_4O_2S:Yb,Tm-based nanoprobe.[199].

Phenols are another important type of exogenous biological reductants other than ascorbates, which are important as dietary supplements and pharmaceuticals. Wang *et al.* reported the detection of chlorogenic acid and oligomeric procyanidins using a square acid-Fe(III) complex-functionalized $NaYF_4$:Yb,Tm nanoprobe.[200] The polyphenols can reduce Fe^{3+} in the complex, decrease the IFE effect, and induce the recovery of fluorescence. However, it suffered from the interference of stronger biological reductants, such as reduced glutathione and ascorbic acid, resulting in poor selectivity of this nanoprobe.

4. Summary and conclusion

The above examples show that different types of inorganic fluorescent nanoprobes have their own specific advantages. First, we compared their fluorescence properties by counting their excitation and emission wavelengths. In terms of excitation wavelengths, the vast majority of redox-responsive lanthanide-doped nanoprobes are excited in the NIR region, whereas the excitation wavelengths of QDs and NCs are generally distributed in the visible region (Fig. 11A). In contrast, the primary fluorescence emission ranges of the three probes are essentially the same (Fig. 11B). It is noteworthy that lanthanide-based systems can only be excited at a few specific wavelengths, which have a similar semi-linear character as their emission. This is mainly caused by the discontinuity in the 4f electronic energy level of the lanthanide ions. Therefore, QDs and NCs are more flexible, with continuously tunable excitation and emission wavelengths, and are relatively more user-friendly. Considering the fact that tissues scatter and absorb NIR light weakly and that the majority of biomolecules do not fluoresce under NIR excitation, lanthanide-doped nanoprobes are more conducive to the detection of redox molecules *in vivo*, enabling diagnostic and imaging-guided tumor therapy. For diagnostics at the level of biological fluids, cells, and tissue sections, QDs and NCs are more practical, largely due to the fact that instruments such as commercially available microplate readers, flow cytometers, and microscopes are commonly equipped with visible light excitation sources. Fig. 12.

In addition, we have performed statistical analyses on the response mechanisms of the different nanoprobes. The response mechanisms of lanthanide-doped nanoprobes are mainly FRET and DS, both of which mainly rely on the energy transfer between lanthanide ions and nearby response groups. Therefore, lanthanide-doped nanoprobes are often nanocomposites containing a pair of rare-earth doped energy donors and energy acceptors modified on the surface. A similar situation occurs for QDs, but so far, no redox-responsive QD nanoprobes based on the DS principle have been reported, which could be a direction for future research. Since QDs and NCs generally contain metal monomers or non-metal anions that are susceptible to oxidation, they can be used to

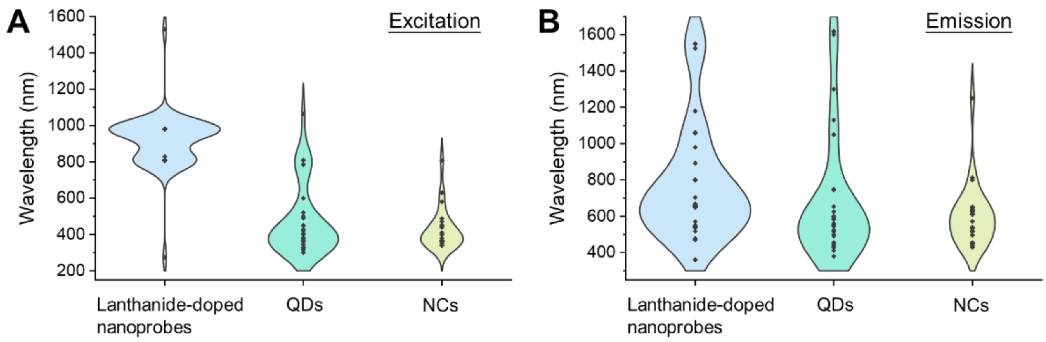

Fig. 11. Excitation (A) and emission wavelength (B) distributions of lanthanide-doped nanoprobes, QDs, and NCs included in this review, based on the data presented in Tables S1 – S8.

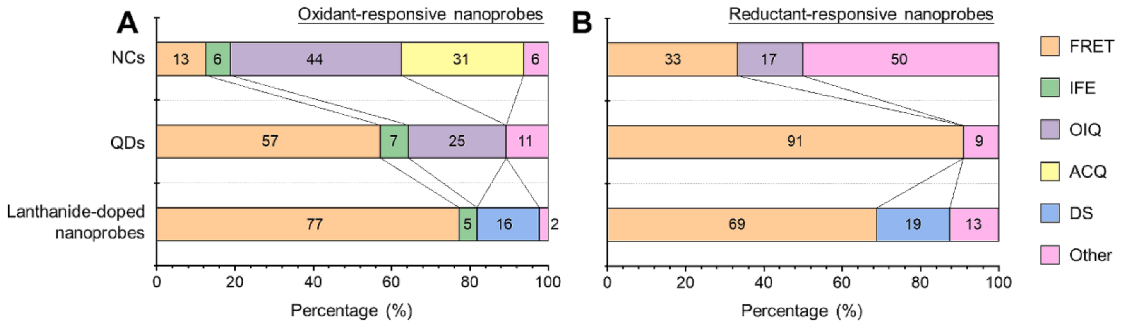

Fig. 12. Response mechanisms of oxidant-responsive (A) and reductant-responsive nanoprobes (B) included in this review, based on the data presented in Tables S1 – S8. FRET: Fluorescence resonance energy transfer; IFE: Inner filter effect; OIQ: Oxidation-induced quenching; ACQ: Aggregation-caused quenching; DS: Dye-sensitizing.

construct responsive probes based on the OIQ mechanism. Since lanthanide-doped nanoprobes are generally chemically stable and typically not undergo redox reactions, OIQ-based construction of lanthanide-doped nanoprobes has not been reported so far. However, some lanthanide ions, such as cerium ions, are able to participate in redox reactions and affect the fluorescence of other lanthanide ions through cross-relaxation during valence changes. Therefore, the development of OIQ-based lanthanide-doped nanoprobes should also be possible. However, the monomers or ions in the probes are oxidized during the OIQ process, accompanied by the risk of potential heavy metal ion leakage. Therefore, the biosafety of this class of OIQ-based nanoprobes needs to be further evaluated. Overall, the redox response mechanism of NCs is richer than that of lanthanide-doped nanoprobes and QDs. This not only makes it easier to develop redox-responsive NCs, but also points a route to use these mechanisms to develop novel redox-responsive lanthanide-doped nanoprobes and QDs.

In short, the advantages of these three probes can be summarized as follows: (1) Lanthanide-doped nanoprobes can be excited by the near-infrared light and emit semi-linear fluorescence, which benefits *in vivo* bioimaging. (2) QDs are rather inexpensive and have tunable excitation and emission wavelengths, which is favorable for practical application. (3) NCs show different mechanisms in response to various analytes, which brings great opportunity to construct nanoplatforms for orthogonal and multiplexed detection.

5. Perspective

In this review, we have summarized recent advances in biological oxidant- and reductant-responsive inorganic fluorescent nanoprobes for diagnostics and treatment. Due to their stable but tunable chemical/physical properties, inorganic fluorescent nanoprobes are favorable for bioapplications as they can meet the challenges of complex biological conditions·H_2O_2-responsive nanoprobes have the highest translational potential for clinical serodiagnostics compared to other oxidant-responsive nanoprobes due to the short lifetime of •OH, ClO^-, and $ONOO^-$ in biofluids. In the future, these nanoprobes may replace H_2O_2-responsive indicators in commercially available kits (*e.g.*, TMB in enzyme-linked immunosorbent assays), since they can also be used with enzymes to detect a wide range of other biomolecules to diagnose related diseases. Furthermore, most reductant-responsive nanoprobes have potential for clinical serodiagnostic applications. While redox-responsive inorganic fluorescent nanoprobes have translational value for *in vivo* imaging, further systematic studies are required to assess their biocompatibility, particularly with regards to nanotoxicity.

To choose an appropriate nanoprobe for a specific application, there is more to consider besides its stability in biosystems such as sensitivity and selectivity to target molecules, reliability and reproducibility of the results, as well as applicability in real practice. For *in vivo* applications, their morphology, surface modification, biocompatibility, and metabolism should also be taken into consideration. Therefore, although much attention has been paid to this topic in the last decades, redox-responsive inorganic fluorescent nanoprobes still need in-depth exploration to attain usefulness in clinical applications. Here, we would like to define and recommend future studies regarding redox-responsive inorganic fluorescent nanoprobes and related bioapplications. The field would greatly benefit from addressing the following questions and challenges.

1) The current selection of fluorescent materials is mainly limited to rare earth nanomaterials, oxide quantum dots, and noble metal nanoclusters, while other materials are less frequently used to construct nanoprobes, such as chalcogenide quantum dots with excellent fluorescence performance and inexpensive non-rare earth transition metal doped materials. An expanded material system will provide more options for probe construction to target different biological applications and meet different application requirements.

2) Much of the current work emphasizes probe sensitivity and pays less attention to selectivity. However, when assessing diagnostic accuracy, too much sensitivity can lead to an increased rate of false positives in the diagnosis. Therefore, equal attention should be given to both in studies. The current redox-responsive nanoprobes suffer from low selectivity because most focus only on their redox property. Therefore, more attention should be paid to the characteristic properties of the molecule other than redox properties. Synergistic determination will be beneficial to obtain better selectivity. For those with extremely similar chemical structures (*e.g.*, Cys and Hcy), attention could be paid to the structural stability of the intermediate formed between them and the recognition group (*e.g.* ring strain).
3) A major advantage of inorganic fluorescent nanoprobes is their ability to provide real-time information through fluorescence imaging, but most current probes require minute or hourly response times, making it difficult to monitor and track molecules. Therefore, the development of probes with fast response performance can highlight the advantage of inorganic fluorescent nanoprobes. Specifically, for organic responsive recognition groups, such as •OH-responsive cyanine skeletons, the electron density should be increased as well as the reactivity with hydroxyl radicals by functional group modification. In addition, by combining high-throughput screening techniques and machine learning, improved reactivity and response times of the recognition groups can be predicted.
4) For the application of redox-responsive inorganic fluorescent nanoprobes in imaging-guided treatment of tumors, current work has focused on the construction of novel nanoprobes, while the interaction between nanoprobes and tumors has been less studied. For example, it is important to know how the levels of redox molecules change over time when the nanoprobes react with them and how this change affects the proliferation and metabolism of tumor cells. In addition, redox molecules are not only markers of the tumor microenvironment, but also have implications in a number of other diseases such as inflammation, infection, and diabetes. Therefore, nanoprobes may also be used in imaging-guided therapies for diseases other than cancer and deserve to be explored in future work.
5) There is a lack of systematic studies on biocompatibility, distribution and metabolism of the probes. Although some work has initially investigated rare earth nanomaterials, quantum dots and clusters, their biological behavior may be different as the surface properties of the probes become more complex after modification with recognition groups. Therefore, studying the biological behavior of probes will improve bioavailability and benefit biological applications, especially therapeutic applications.
6) For those H_2O_2-responsive nanoprobes used for various biomolecular assays based on enzymatic reactions, endogenous H_2O_2 will affect the assay results and increase the false-positive rates of diagnosis. Although it is currently possible to remove endogenous H_2O_2 by adding peroxidase or reducing agents, this adds cost and complexity to the assay system. Therefore, the ability to avoid the interference of endogenous H_2O_2 by establishing an internal reference specifically for H_2O_2 or other means will be key to determining the clinical reliability of this type of nanoprobes.

Author contributions.

Y.L. and Z.W. organized the reference list. Y.L. wrote the original manuscript. All authors decided the topic and the visualization. All authors contributed to the review and editing of manuscript.

CRediT authorship contribution statement

Yuxin Liu: Conceptualization, Visualization, Writing – original draft. **Zheng Wei:** Conceptualization, Visualization, Funding acquisition, Writing – review & editing. **Francesco F. Mutti:** Conceptualization, Visualization, Funding acquisition, Writing – review & editing. **Hong Zhang:** Conceptualization, Visualization, Funding acquisition, Writing – review & editing. **Felix F. Loeffler:** Conceptualization, Visualization, Funding acquisition, Writing – review & editing.

Declaration of competing interest

The authors declare that they have no known competing financial interests or personal relationships that could have appeared to influence the work reported in this paper.

Data availability

Data is available in the supporting information.

Acknowledgements

The authors acknowledge the financial support from the German Federal Ministry of Education and Research (BMBF, 13XP5050A, F.F.L.), the Max-Planck-Fraunhofer collaborative project (Glyco3Display, F.F.L.), the Max Planck Society, NWO Sector Plan for Physics and Chemistry (F.G.M.), EU H2020-MSCA-RISE-2017 Action program (CANCER, 777682, H.Z.), and the China Scholarship Council scholarship (202008110184, Z.W.).

Appendix A. Supplementary data

Supplementary data to this article can be found online at https://doi.org/10.1016/j.ccr.2024.215817.

References

[1] B. Korac, A. Kalezic, V. Pekovic-Vaughan, A. Korac, A. Jankovic, Redox changes in obesity, metabolic syndrome, and diabetes, Redox Biol. 42 (2021) 101887.
[2] J. Zuo, Z. Zhang, M.C. Luo, L. Zhou, E.C. Nice, W. Zhang, C. Wang, C.H. Huang, Redox signaling at the crossroads of human health and disease, MedComm 3 (2) (2022) e127.
[3] G. Bartosz, Reactive oxygen species: destroyers or messengers? Biochem. Pharmacol. 77 (8) (2009) 1303–1315.
[4] J. Pourova, M. Kottova, M. Voprsalova, M. Pour, Reactive oxygen and nitrogen species in Normal physiological processes, Acta Physiol. 198 (1) (2010) 15–35.
[5] M. Valko, K. Jomova, C.J. Rhodes, K. Kuca, K. Musilek, Redox- and non-redox-metal-induced formation of free radicals and their role in human disease, Arch. Toxicol. 90 (1) (2016) 1–37.
[6] C.M. Bergamini, S. Gambetti, A. Dondi, C. Cervellati, Oxygen, reactive oxygen species and tissue damage, Curr. Pharm. Des. 10 (14) (2004) 1611–1626.
[7] Z. Fatehi-Hassanabad, C.B. Chan, B.L. Furman, Reactive oxygen species and endothelial function in diabetes, Eur. J. Pharmacol. 636 (1) (2010) 8–17.
[8] K. Sugamura, J.F. Keaney, Reactive oxygen species in Cardiovascular disease, Free Radic. Biol. Med. 51 (5) (2011) 978–992.
[9] S.S. Garg, J. Gupta, Polyol pathway and redox balance in diabetes, Pharmacol. Res. 182 (2022) 106326.
[10] M. Fransen, C. Lismont, Redox signaling from and to Peroxisomes: Progress, challenges, and prospects, Antioxid. Redox Signal. 30 (1) (2018) 95–112.
[11] K. Van Laer, C.J. Hamilton, J. Messens, Low-Molecular-weight thiols in thiol-disulfide exchange, Antioxid. Redox Signal. 18 (13) (2013) 1642–1653.
[12] W. Ying, Nad+/Nadh and Nadp+/Nadph in Cellular functions and cell death: regulation and biological consequences, Antioxid. Redox Signal. 10 (2) (2007) 179–206.
[13] Y. Yano, Flavin chemistry with oxidation-active flavin mimics and receptors, Rev. Heteroat. Chem. 22 (2000) 151–179.
[14] C.C. Winterbourn, M.B. Hampton, Thiol chemistry and specificity in redox signaling, Free Radic. Biol. Med. 45 (5) (2008) 549–561.
[15] M.M.E. Huijbers, S. Montersino, A.H. Westphal, D. Tischler, W.J.H. van Berkel, Flavin dependent monooxygenases, Arch. Biochem. Biophys. 544 (2014) 2–17.
[16] J.F. Gregory III, Ascorbic acid bioavailability in foods and supplements, Nutr. Rev. 51 (10) (1993) 301–303.
[17] H.N. Rajha, A. Paule, G. Aragonès, M. Barbosa, C. Caddeo, E. Debs, R. Dinkova, G. P. Eckert, A. Fontana, P. Gebrayel, R.G. Maroun, A. Napolitano, L. Panzella, G. M. Pasinetti, J.F. Stevens, A. Schieber, M. Edeas, Recent advances in Research on polyphenols: effects on Microbiota, metabolism, and health, Mol. Nutr. Food Res. 66 (1) (2022) e2100670.
[18] Y. Lei, K. Wang, L. Deng, Y. Chen, E.C. Nice, C. Huang, Redox regulation of inflammation: old elements, a new story, Med. Res. Rev. 35 (2) (2015) 306–340.
[19] P. Adhya, S.S. Sharma, Redox trps in diabetes and diabetic complications: mechanisms and Pharmacological modulation, Pharmacol. Res. 146 (2019) 104271.

[20] K.K. Galougahi, C. Antoniades, S.J. Nicholls, K.M. Channon, G.A. Figtree, Redox Biomarkers in Cardiovascular medicine, Eur. Heart J. 36 (25) (2015) 1576–1582.
[21] G.J. McBean, M. Aslan, H.R. Griffiths, R.C. Torrão, Thiol redox homeostasis in neurodegenerative disease, Redox Biol. 5 (2015) 186–194.
[22] H.J. Park, E. Mah, R.S. Bruno, Validation of high-performance liquid chromatography–boron-doped diamond detection for assessing hepatic glutathione redox status, Anal. Biochem. 407 (2) (2010) 151–159.
[23] E. Dervisevic, N.H. Voelcker, G. Risbridger, K.L. Tuck, V.J. Cadarso, Colorimetric detection of Extracellular hydrogen peroxide using an integrated microfluidic Device, Anal. Chem. 94 (3) (2022) 1726–1732.
[24] C. Hung Tzang, R. Yuan, M. Yang, Voltammetric biosensors for the determination of formate and Glucose-6-phosphate based on the measurement of dehydrogenase-generated nadh and nadph, Biosens. Bioelectron. 16 (3) (2001) 211–219.
[25] D. Semeniak, D.F. Cruz, A. Chilkoti, M.H. Mikkelsen, Plasmonic fluorescence enhancement in diagnostics for clinical tests at point-of-Care: a review of recent technologies, Adv. Mater. 35 (34) (2022) e2107986.
[26] B.A. Kairdolf, A.M. Smith, T.H. Stokes, M.D. Wang, A.N. Young, S. Nie, Semiconductor quantum dots for bioimaging and biodiagnostic applications, Annu. Rev. Anal. Chem. 6 (1) (2013) 143–162.
[27] E. Song, M. Chen, Z. Chen, Y. Zhou, W. Zhou, H.-T. Sun, X. Yang, J. Gan, S. Ye, Q. Zhang, Mn2+-activated dual-wavelength emitting materials toward Wearable optical fibre temperature sensor, Nat. Commun. 13 (1) (2022) 2166.
[28] R.L. Pinals, F. Ledesma, D. Yang, N. Navarro, S. Jeong, J.E. Pak, L. Kuo, Y.-C. Chuang, Y.-W. Cheng, H.-Y. Sun, M.P. Landry, Rapid Sars-Cov-2 spike protein detection by Carbon nanotube-based near-Infrared nanosensors, Nano Lett. 21 (5) (2021) 2272–2280.
[29] L. Zhou, Y. Fan, R. Wang, X. Li, L. Fan, F. Zhang, High-capacity upconversion wavelength and lifetime Binary encoding for multiplexed biodetection, Angew. Chem. Int. Ed. 57 (39) (2018) 12824–12829.
[30] Q. Yu, L. Xue, J. Hiblot, R. Griss, S. Fabritz, C. Roux, P.-A. Binz, D. Haas, J. G. Okun, K. Johnsson, Semisynthetic sensor proteins enable metabolic assays at the point of Care, Science 361 (6407) (2018) 1122–1126.
[31] J. Wang, C. Jiang, J. Jin, L. Huang, W. Yu, B. Su, J. Hu, Ratiometric fluorescent lateral flow immunoassay for point-of-Care testing of acute Myocardial Infarction, Angew. Chem. Int. Ed. 60 (23) (2021) 13042–13049.
[32] T. Xu, C. Liang, S. Ji, D. Ding, D. Kong, L. Wang, Z. Yang, Surface-induced hydrogelation for fluorescence and naked-eye detections of enzyme activity in blood, Anal. Chem. 88 (14) (2016) 7318–7323.
[33] E.M. Sevick-Muraca, Translation of near-Infrared fluorescence imaging technologies: Emerging clinical applications, Annu. Rev. Med. 63 (1) (2012) 217–231.
[34] J.A. Carr, D. Franke, J.R. Caram, C.F. Perkinson, M. Saif, V. Askoxylakis, M. Datta, D. Fukumura, R.K. Jain, M.G. Bawendi, O.T. Bruns, Shortwave Infrared fluorescence imaging with the clinically approved near-Infrared dye indocyanine green, Proc. Natl. Acad. Sci. u.s.a. 115 (17) (2018) 4465–4470.
[35] T.F. Zhang, Y.Y. Li, Z. Zheng, R.Q. Ye, Y.R. Zhang, R.T.K. Kwok, J.W.Y. Lam, B. Z. Tang, In situ monitoring apoptosis process by a self-reporting photosensitizer, J. Am. Chem. Soc. 141 (14) (2019) 5612–5616.
[36] L. Wu, A.C. Sedgwick, X. Sun, S.D. Bull, X.-P. He, T.D. James, Reaction-based fluorescent probes for the detection and imaging of reactive oxygen, nitrogen, and sulfur species, Acc. Chem. Res. 52 (9) (2019) 2582–2597.
[37] S.Y. Park, S.A. Yoon, Y. Cha, M.H. Lee, Recent advances in fluorescent probes for Cellular antioxidants: detection of nadh, hnqo 1, H2s, and other redox biomolecules, Coordin. Chem. Rev. 428 (2021) 213613.
[38] U. Resch-Genger, M. Grabolle, S. Cavaliere-Jaricot, R. Nitschke, T. Nann, Quantum dots versus organic dyes as fluorescent labels, Nat. Methods 5 (9) (2008) 763–775.
[39] W.C.W. Chan, D.J. Maxwell, X. Gao, R.E. Bailey, M. Han, S. Nie, Luminescent quantum dots for multiplexed biological detection and imaging, Curr. Opin. Biotechnol. 13 (1) (2002) 40–46.
[40] T. Ha, P. Tinnefeld, Photophysics of fluorescent probes for single-molecule biophysics and super-resolution imaging, Annu. Rev. Phys. Chem. 63 (1) (2012) 595–617.
[41] M. Levitus, S. Ranjit, Cyanine dyes in biophysical Research: the photophysics of polymethine fluorescent dyes in Biomolecular environments, Q. Rev. Biophys. 44 (1) (2011) 123–151.
[42] E. Babu, J. Bhuvaneswari, P. Muthu Mareeswaran, P. Thanasekaran, H.-M. Lee, S. Rajagopal, Transition metal complexes based Aptamers as optical diagnostic tools for disease proteins and biomolecules, Coordin. Chem. Rev. 380 (2019) 519–549.
[43] W. Liu, J. Chen, Z. Xu, Fluorescent probes for biothiols based on metal complex, Coordin. Chem. Rev. 429 (2021) 213638.
[44] E. Pershagen, K.E. Borbas, Designing reactivity-based responsive lanthanide probes for multicolor detection in biological systems, Coordin. Chem. Rev. 273–274 (2014) 30–46.
[45] Z. Li, H. Yuan, W. Yuan, Q. Su, F. Li, Upconversion nanoprobes for biodetections, Coordin. Chem. Rev. 354 (2018) 155–168.
[46] T.F. Anjong, H. Choi, J. Yoo, Y. Bak, Y. Cho, D. Kim, S. Lee, K. Lee, B.-G. Kim, S. Kim, Multifunction-Harnessed afterglow nanosensor for Molecular imaging of acute kidney injury in vivo, Small 18 (22) (2022) 2200245.
[47] M.T. Abbas, N.Z. Khan, J. Mao, L. Qiu, X. Wei, Y. Chen, S.A. Khan, Lanthanide and transition metals doped materials for non-contact optical thermometry with promising approaches, Mater. Today Chem. 24 (2022) 100903.
[48] S. Christ, M. Schaferling, Chemical sensing and imaging based on photon upconverting Nano- and Microcrystals: a review, Methods Appl. Fluoresc. 3 (3) (2015) 034004.
[49] Q. Su, W. Feng, D. Yang, F. Li, Resonance energy transfer in upconversion nanoplatforms for selective biodetection, Acc. Chem. Res. 50 (1) (2017) 32–40.
[50] Y. Liu, Z. Wei, X. Liao, J. Zhou, Multichannel lanthanide-doped nanoprobes improve diagnostic performance, Acc. Mater. Res. 1 (3) (2020) 225–235.
[51] J. Zheng, C. Zhou, M. Yu, J. Liu, Different sized luminescent gold Nanoparticles, Nanoscale 4 (14) (2012) 4073–4083.
[52] A.L. Efros, L.E. Brus, Nanocrystal quantum dots: from discovery to modern development, ACS Nano 15 (4) (2021) 6192–6210.
[53] M. Richter, Nanoplatelets as material system between strong confinement and weak confinement, Phys. Rev. Mater. 1 (1) (2017) 016001.
[54] L.E. Brus, Electron-electron and electron-hole Interactions in small semiconductor crystallites: the size dependence of the lowest excited electronic state, J. Chem. Phys. 80 (9) (1984) 4403–4409.
[55] R. Rossetti, S. Nakahara, L.E. Brus, Quantum size effects in the redox potentials, resonance raman spectra, and electronic spectra of cds crystallites in aqueous solution, J. Chem. Phys. 79 (2) (1983) 1086–1088.
[56] V. Jungnickel, F. Henneberger, Luminescence related processes in semiconductor nanocrystals —the strong confinement regime, J. Lumin. 70 (1) (1996) 238–252.
[57] Y. Zhang, T.-H. Wang, Quantum dot enabled Molecular sensing and diagnostics, Theranostics 2 (7) (2012) 631–654.
[58] S.M. van de Looij, E.R. Hebels, M. Viola, M. Hembury, S. Oliveira, T. Vermonden, Gold nanoclusters: imaging, therapy, and theranostic roles in biomedical applications, Bioconjug. Chem. 33 (1) (2022) 4–23.
[59] H. Park, D.J. Shin, J. Yu, Categorization of quantum dots, clusters, nanoclusters, and nanodots, J. Chem. Edu. 98 (3) (2021) 703–709.
[60] S. Chinnathambi, S. Chen, S. Ganesan, N. Hanagata, Silicon quantum dots for biological applications, Adv. Healthcare Mater. 3 (1) (2014) 10–29.
[61] M.-M. Zhang, K. Li, S.-Q. Zang, Progress in atomically Precise coinage metal clusters with aggregation-induced emission and Circularly Polarized luminescence, Adv. Opt. Mater. 8 (14) (2020) 1902152.
[62] U. Gupta, V. Gupta, R.K. Arun, N. Chanda, Recent advances in enzymatic biosensors for point-of-Care detection of biomolecules, Biotechnol. Bioeng. 119 (12) (2022) 3393–3407.
[63] E.S. Speranskaya, D.D. Drozd, P.S. Pidenko, I.Y. Goryacheva, Enzyme modulation of quantum dot luminescence: application in bioanalysis, Trends Analyt. Chem. 127 (2020) 115897.
[64] Dizdaroglu, M.; Jaruga, P.; Birincioglu, M.; Rodriguez, H., Free Radical-Induced Damage to DNA: Mechanisms and Measurement1, 2 1this Article Is Part of a Series of Reviews on "Oxidative DNA Damage and Repair." the Full List of Papers May Be Found on the Homepage of the Journal. 2guest Editor: Miral Dizdaroglu. *Free Radic. Biol. Med.* **2002,** *32* (11), 1102-1115.
[65] A.M. Fleming, C.J. Burrows, On the Irrelevancy of hydroxyl radical to DNA damage from oxidative stress and implications for epigenetics, Chem. Soc. Rev. 49 (18) (2020) 6524–6528.
[66] P. Katakwar, R. Metgud, S. Naik, R. Mittal, Oxidative stress Marker in Oral cancer: a review, J. Cancer Res. Ther. 12 (2) (2016) 438–446.
[67] A.K. Saini, R.J. Patel, S.S. Sharma, H.S., A.K., Edaravone attenuates hydroxyl radical stress and augmented angiotensin ii response in diabetic rats, Pharmacol. Res. 54 (1) (2006) 6–10.
[68] D. Matuz-Mares, H. Riveros-Rosas, M.M. Vilchis-Landeros, H. Vázquez-Meza, Glutathione Participation in the prevention of Cardiovascular diseases, Antioxidants 10 (8) (2021) 1220.
[69] T. Obata, Environmental estrogen-like chemicals and hydroxyl radicals induced by mptp in the striatum: a review, Neurochem. Res. 27 (5) (2002) 423–431.
[70] P. Attri, Y.H. Kim, D.H. Park, J.H. Park, Y.J. Hong, H.S. Uhm, K.-N. Kim, A. Fridman, E.H. Choi, Generation mechanism of hydroxyl radical species and its lifetime prediction during the plasma-initiated ultraviolet (uv) photolysis, Sci. Rep. 5 (1) (2015) 9332.
[71] Q. Mei, Y. Li, B.N. Li, Y. Zhang, Oxidative cleavage-based upconversional nanosensor for visual evaluation of antioxidant activity of drugs, Biosensor. Bioelectron. 64 (2015) 88–93.
[72] Z. Li, T. Liang, S. Lv, Q. Zhuang, Z. Liu, A rationally designed upconversion nanoprobe for in vivo detection of hydroxyl radical, J. Am. Chem. Soc. 137 (34) (2015) 11179–11185.
[73] X.Y. Song, J.Y. Zhang, Z.H. Yue, Z.H. Wang, Z.H. Liu, S.S. Zhang, Dual-activator codoped upconversion nanoprobe with Core - multishell structure for in vitro and in vivo detection of hydroxyl radical, Anal. Chem. 89 (20) (2017) 11021–11026.
[74] G. Yu, N. Feng, D. Zhao, H. Wang, Y. Jin, D. Liu, Z. Li, X. Yang, K. Ge, J. Zhang, A highly selective and sensitive upconversion nanoprobe for monitoring hydroxyl radicals in living cells and the liver, Sci. China Life Sci. 64 (3) (2021) 434–442.
[75] Q. Guo, Y. Liu, Q. Jia, G. Zhang, H. Fan, L. Liu, J. Zhou, Ultrahigh sensitivity multifunctional nanoprobe for the detection of hydroxyl radical and evaluation of heavy metal induced oxidative stress in live hepatocyte, Anal. Chem. 89 (9) (2017) 4986–4993.
[76] Q. Jia, Y. Liu, Y. Duan, J. Zhou, Interference-free detection of hydroxyl radical and arthritis diagnosis by Rare Earth-based nanoprobe utilizing swir emission as reference, Anal. Chem. 91 (17) (2019) 11433–11439.
[77] Y. Liu, Q. Jia, Q. Guo, A. Jiang, J. Zhou, In vivo oxidative stress monitoring through Intracellular hydroxyl radicals detection by recyclable upconversion nanoprobes, Anal. Chem. 89 (22) (2017) 12299–12305.
[78] W. Zhou, Y. Cao, D. Sui, C. Lu, Turn-on luminescent probes for the real-time monitoring of endogenous hydroxyl radicals in living cells, Angew. Chem. Int. Ed. 55 (13) (2016) 4236–4241.

[79] Y.-C. Sun, L.-F. Pang, X.-F. Guo, H. Wang, Synthesis of metal ion-tolerant mn-doped fluorescence silicon quantum dots with green emission and its application for selective imaging of ·oh in living cells, Microchim. Acta 189 (2) (2022) 60.
[80] J. Tan, Y. Song, X. Dai, G. Wang, L. Zhou, One-pot synthesis of robust dendritic sulfur quantum dots for two-photon fluorescence imaging and "off–on" detection of hydroxyl radicals and ascorbic acid, Nanoscale Adv. 4 (19) (2022) 4035–4040.
[81] F. Liu, T. Bing, D. Shangguan, M. Zhao, N. Shao, Ratiometric fluorescent biosensing of hydrogen peroxide and hydroxyl radical in living cells with lysozyme-silver nanoclusters: lysozyme as stabilizing ligand and fluorescence signal unit, Anal. Chem. 88 (21) (2016) 10631–10638.
[82] J. Li, J. Yu, Y. Huang, H. Zhao, L. Tian, Highly stable and multiemissive silver nanoclusters synthesized in situ in a DNA hydrogel and their application for hydroxyl radical sensing, ACS Appl. Mater. Interfaces 10 (31) (2018) 26075–26083.
[83] W. Mi, S. Tang, Y. Jin, N. Shao, Au/Ag Bimetallic nanoclusters stabilized by glutathione and lysozyme for ratiometric sensing of H2o2 and hydroxyl radicals, ACS Appl. Nano Mater. 4 (2) (2021) 1586–1595.
[84] Y. You, S. Cheng, L. Zhang, Y. Zhu, C. Zhang, Y. Xian, Rational modulation of the luminescence of upconversion nanomaterials with phycocyanin for the sensing and imaging of myeloperoxidase during an inflammatory process, Anal. Chem. 92 (7) (2020) 5091–5099.
[85] Q. Mei, W. Deng, W. Yisibashaer, H. Jing, G. Du, M. Wu, B.N. Li, Y. Zhang, Zinc-dithizone complex engineered upconverting nanosensors for the detection of hypochlorite in living cells, Small 11 (35) (2015) 4568–4575.
[86] R. Zhang, L. Liang, Q. Meng, J. Zhao, H.T. Ta, L. Li, Z. Zhang, Y. Sultanbawa, Z. P. Xu, Responsive upconversion nanoprobe for background-free hypochlorous acid detection and bioimaging, Small 15 (2) (2019) 1803712.
[87] F. Wang, X. Qu, D. Liu, C. Ding, C. Zhang, Y. Xian, Upconversion Nanoparticles-Mos2 nanoassembly as a fluorescent turn-on probe for bioimaging of reactive oxygen species in living cells and zebrafish, Sensor. Actuat. B - Chem. 274 (2018) 180–187.
[88] L. Liu, G. Zhu, W. Zeng, B. Lv, Y. Yi, Highly sensitive and selective "off-on" fluorescent sensing platform for Clo− in water based on silicon quantum dots coupled with nanosilver, Anal. Bioanal. Chem. 411 (8) (2019) 1561–1568.
[89] Y. Zha, R. Xin, M. Zhang, X. Cui, N. Li, Stimuli-responsive azobenzene-quantum dots for multi-sensing of dithionite, hypochlorite, and azoreductase, Microchim. Acta 187 (8) (2020) 481.
[90] M. Liu, Y. Bai, Y. He, J. Zhou, Y. Ge, J. Zhou, G. Song, Facile microwave-assisted synthesis of Ti3c2 mxene quantum dots for ratiometric fluorescence detection of hypochlorite, Microchim. Acta 188 (1) (2021) 15.
[91] X. Zou, Y. Liu, X. Zhu, M. Chen, L. Yao, W. Feng, F. Li, An Nd3+-sensitized upconversion nanophosphor modified with a cyanine dye for the ratiometric upconversion luminescence bioimaging of hypochlorite, Nanoscale 7 (9) (2015) 4105–4113.
[92] M. Zhang, M. Zuo, C. Wang, Z. Li, Q. Cheng, J. Huang, Z. Wang, Z. Liu, Monitoring neuroinflammation with an hocl-activatable and blood-brain Barrier permeable upconversion nanoprobe, Anal. Chem. 92 (7) (2020) 5569–5576.
[93] J. Ke, S. Lu, X. Shang, Y. Liu, H. Guo, W. You, X. Li, J. Xu, R. Li, Z. Chen, X. Chen, A strategy of nir dual-excitation upconversion for ratiometric Intracellular detection, Adv. Sci. 6 (22) (2019) 1901874.
[94] P. Zhang, J. Ke, D. Tu, J. Li, Y. Pei, L. Wang, X. Shang, T. Guan, S. Lu, Z. Chen, X. Chen, Enhancing dye-triplet-sensitized upconversion emission through the heavy-atom effect in Cslu2f7:Yb/Er nanoprobes, Angew. Chem. Int. Ed. 61 (1) (2022) e202112125.
[95] X. Zou, X. Zhou, C. Cao, W. Lu, W. Yuan, Q. Liu, W. Feng, F. Li, Dye-sensitized upconversion nanocomposites for ratiometric semi-quantitative detection of hypochlorite in vivo, Nanoscale 11 (6) (2019) 2959–2965.
[96] J. Ke, S. Lu, Z. Li, X. Shang, X. Li, R. Li, D. Tu, Z. Chen, X. Chen, Multiplexed Intracellular detection based on dual-excitation/dual-emission upconversion nanoprobes, Nano Res. 13 (7) (2020) 1955–1961.
[97] M. Wang, R. Mi, L. Wang, H. Chen, Preparation of cyanine dye sensitized upconversion luminescent nanoprobe and hypochlorous acid detection by light-emitting energy transfer, J. Luminescence 239 (2021) 118395.
[98] S. Wang, L. Liu, Y. Fan, A.M. El-Toni, M.S. Alhoshan, D. Li, F. Zhang, In vivo high-resolution ratiometric fluorescence imaging of inflammation using nir-ii nanoprobes with 1550 nm emission, Nano Lett. 19 (4) (2019) 2418–2427.
[99] P. Pei, H. Hu, Y. Chen, S. Wang, J. Chen, J. Ming, Y. Yang, C. Sun, S. Zhao, F. Zhang, Nir-ii ratiometric lanthanide-dye hybrid nanoprobes doped bioscaffolds for in situ bone repair monitoring, Nano Lett. 22 (2) (2022) 783–791.
[100] M.C. Mancini, B.A. Kairdolf, A.M. Smith, S. Nie, Oxidative quenching and degradation of Polymer-encapsulated quantum dots: new insights into the long-term fate and toxicity of nanocrystals in vivo, J. Am. Chem. Soc. 130 (33) (2008) 10836–10837.
[101] Y. Yan, S. Wang, Z. Liu, H. Wang, D. Huang, Cdse-zns quantum dots for selective and sensitive detection and quantification of hypochlorite, Anal. Chem. 82 (23) (2010) 9775–9781.
[102] K. Singh, S.K. Mehta, Luminescent zno quantum dots as an efficient sensor for free chlorine detection in water, Analyst 141 (8) (2016) 2487–2492.
[103] Y. Wang, P. Zhang, Q. Lu, Y. Wang, W. Fu, Q. Tan, W. Luo, Water-soluble Mos2 quantum dots are a viable fluorescent probe for hypochlorite, Microchim. Acta 185 (4) (2018) 233.
[104] H. Yang, Q. Zhao, X. Wang, Y. Wu, Y. Su, W. Wei, Facile and highly selective sensing of hypochlorous acid in aqueous solution and living cells by using as-Prepared Wse2 quantum dots, Sensor. Actuat. B - Chem. 337 (2021) 129782.
[105] Y. Guo, L. Zhang, F. Cao, L. Mang, X. Lei, S. Cheng, J. Song, Hydrothermal synthesis of blue-emitting silicon quantum dots for fluorescent detection of hypochlorite in tap water, Anal. Methods 8 (13) (2016) 2723–2728.
[106] S. Park, S. Choi, J. Yu, DNA-encapsulated silver nanodots as ratiometric luminescent probes for hypochlorite detection, Nanoscale Res. Lett. 9 (1) (2014) 129.
[107] Q. Tang, T. Yang, Y. Huang, Copper nanocluster-based fluorescent probe for hypochlorite, Microchim. Acta 182 (13) (2015) 2337–2343.
[108] X. Xiong, Y. Tang, L. Zhang, S. Zhao, A label-free fluorescent assay for free chlorine in drinking water based on protein-stabilized gold nanoclusters, Talanta 132 (2015) 790–795.
[109] P. Zhang, Y. Wang, L. Chen, Y. Yin, Bimetallic nanoclusters with strong red fluorescence for sensitive detection of hypochlorite in tap water, Microchim. Acta 184 (10) (2017) 3781–3787.
[110] Y. Li, Y. He, Y. Ge, G. Song, J. Zhou, Smartphone-assisted visual ratio-fluorescence detection of hypochlorite based on copper nanoclusters, Spectrochim. Acta A Mol. Biomol. Spectrosc. 255 (2021) 119740.
[111] Y. Zhou, W. Pei, X. Zhang, W. Chen, J. Wu, C. Yao, L. Huang, H. Zhang, W. Huang, J.S. Chye Loo, Q. Zhang, A cyanine-modified upconversion nanoprobe for nir-excited imaging of endogenous hydrogen peroxide signaling in vivo, Biomaterials 54 (2015) 34–43.
[112] H. Wang, Y. Li, M. Yang, P. Wang, Y. Gu, Fret-based upconversion nanoprobe sensitized by Nd3+ for the ratiometric detection of hydrogen peroxide in vivo, ACS Appl. Mater. Interfaces 11 (7) (2019) 7441–7449.
[113] J. Zheng, Y. Wu, D. Xing, T. Zhang, Synchronous detection of glutathione/hydrogen peroxide for monitoring redox status in vivo with a ratiometric upconverting nanoprobe, Nano Res. 12 (4) (2019) 931–938.
[114] P. Singh, P. Singh, R. Prakash, S.B. Rai, Photo-physical studies of ultrasmall upconversion Nanoparticles embedded Organometallic complexes: probing a dual mode optical sensor for hydrogen peroxide, Opt. Mater. 98 (2019) 109459.
[115] L. Liu, S. Wang, B. Zhao, P. Pei, Y. Fan, X. Li, F. Zhang, Er3+ sensitized 1530 nm to 1180 nm second near-Infrared window upconversion nanocrystals for in vivo biosensing, Angew. Chem. Int. Ed. 57 (25) (2018) 7518–7522.
[116] C. Hao, X. Wu, M. Sun, H. Zhang, A. Yuan, L. Xu, C. Xu, H. Kuang, Chiral Core-Shell upconversion Nanoparticle@Mof nanoassemblies for quantification and bioimaging of reactive oxygen species in vivo, J. Am. Chem. Soc. 141 (49) (2019) 19373–19378.
[117] T. Jia, Z. Wang, Q. Sun, S. Dong, J. Xu, F. Zhang, L. Feng, F. He, D. Yang, P. Yang, J. Lin, Intelligent Fe–Mn layered double hydroxides nanosheets anchored with upconversion Nanoparticles for oxygen-elevated synergetic therapy and bioimaging, Small 16 (46) (2020) 2001343.
[118] C. Sun, M. Gradzielski, Upconversion-based nanosystems for fluorescence sensing of ph and H2o2, Nanoscale Adv. 3 (9) (2021) 2538–2546.
[119] W.-L. Wan, B. Tian, Y.-J. Lin, C. Korupalli, M.-Y. Lu, Q. Cui, D. Wan, Y. Chang, H.-W. Sung, Photosynthesis-inspired H2 generation using a chlorophyll-loaded liposomal nanoplatform to detect and scavenge excess ros, Nat. Commun. 11 (1) (2020) 534.
[120] L. Shang, S. Dong, Design of fluorescent assays for cyanide and hydrogen peroxide based on the inner filter effect of metal Nanoparticles, Anal. Chem. 81 (4) (2009) 1465–1470.
[121] O. Adegoke, S. Khene, T. Nyokong, Fluorescence "switch on" of conjugates of cdte@zns quantum dots with al, ni and zn tetraamino-phthalocyanines by hydrogen peroxide: Characterization and applications as luminescent nanosensors, J. Fluoresc. 23 (5) (2013) 963–974.
[122] Q. Zhao, S. Chen, H. Huang, L. Zhang, L. Wang, F. Liu, J. Chen, Y. Zeng, P.K. Chu, Colorimetric and ultra-sensitive fluorescence resonance energy transfer determination of H2o2 and glucose by multi-functional au nanoclusters, Analyst 139 (6) (2014) 1498–1503.
[123] R. Lv, M. Feng, L. Xiao, J.A. Damasco, J. Tian, P.N. Prasad, Multilevel Nanoarchitecture exhibiting biosensing for cancer diagnostics by dual-modal switching of optical and magnetic resonance signals, ACS Appl. Bio Mater. 1 (5) (2018) 1505–1511.
[124] I. Martínez-Reyes, N.S. Chandel, Cancer metabolism: looking Forward, Nat. Rev. Cancer 21 (10) (2021) 669–680.
[125] W. Fan, W. Bu, B. Shen, Q. He, Z. Cui, Y. Liu, X. Zheng, K. Zhao, J. Shi, Intelligent Mno2 nanosheets anchored with upconversion nanoprobes for concurrent ph-/H2o2-responsive ucl imaging and oxygen-elevated synergetic therapy, Adv. Mater. 27 (28) (2015) 4155–4161.
[126] C. Zhang, W.-H. Chen, L.-H. Liu, W.-X. Qiu, W.-Y. Yu, X.-Z. Zhang, An O2 self-supplementing and reactive-oxygen-species-circulating amplified nanoplatform via H2o/H2o2 splitting for tumor imaging and photodynamic therapy, Adv. Funct. Mater. 27 (43) (2017) 1700626.
[127] X. Ai, M. Hu, Z. Wang, L. Lyu, W. Zhang, J. Li, H. Yang, J. Lin, B. Xing, Enhanced Cellular ablation by attenuating hypoxia status and reprogramming tumor-associated macrophages via nir light-responsive upconversion nanocrystals, Bioconjugate Chem. 29 (4) (2018) 928–938.
[128] J. Xu, W. Han, P. Yang, T. Jia, S. Dong, H. Bi, A. Gulzar, D. Yang, S. Gai, F. He, J. Lin, C. Li, Tumor microenvironment-responsive mesoporous Mno2-coated upconversion nanoplatform for self-enhanced tumor theranostics, Adv. Funct. Mater. 28 (36) (2018) 1803804.
[129] R.-G. Wang, M.-Y. Zhao, D. Deng, X. Ye, F. Zhang, H. Chen, J.-L. Kong, An intelligent and biocompatible photosensitizer conjugated silicon quantum Dots–Mno2 nanosystem for fluorescence imaging-guided efficient photodynamic therapy, J. Mater. Chem. B 6 (28) (2018) 4592–4601.
[130] Y.J. Li, H.R. Zhang, Y.Y. Yao, T. Gong, R.Y. Dong, D.N. Li, Y.L. Liu, B.F. Lei, Promoted off-on recognition of H2o2 based on the fluorescence of silicon

quantum dots assembled two-dimensional peg-Mno2 nanosheets hybrid nanoprobe, Microchim. Acta 187 (6) (2020) 347.
[131] M. Wang, H. Li, B. Huang, S. Chen, R. Cui, Z.-J. Sun, M. Zhang, T. Sun, An ultra-stable, oxygen-supply nanoprobe emitting in near-Infrared-ii window to guide and enhance radiotherapy by promoting anti-tumor immunity, Adv. Healthcare Mater. 10 (12) (2021) 2100090.
[132] W. Bai, K. Zhang, S. Yu, J. Zhang, L. Jin, The Preparation of Mno2/Bsa/Cdte quantum dots complex for ratiometric fluorescence/T1-weighted mri detection of H2o2, Talanta 252 (2023) 123774.
[133] H.-B. Wang, Y. Chen, N. Li, Y.-M. Liu, A fluorescent glucose bioassay based on the hydrogen peroxide-induced decomposition of a quencher system composed of Mno2 nanosheets and copper nanoclusters, Microchim. Acta 184 (2) (2017) 515–523.
[134] X. Yan, D. Kong, R. Jin, X. Zhao, H. Li, F. Liu, Y. Lin, G. Lu, Fluorometric and colorimetric analysis of Carbamate pesticide via enzyme-triggered decomposition of gold nanoclusters-anchored Mno2 nanocomposite, Sensor. Actuat. B - Chem. 290 (2019) 640–647.
[135] J. Yuan, Y. Cen, X.-J. Kong, S. Wu, C.-L. Liu, R.-Q. Yu, X. Chu, Mno2-nanosheet-modified upconversion nanosystem for sensitive turn-on fluorescence detection of H2o2 and glucose in blood, ACS Appl. Mater. Interfaces 7 (19) (2015) 10548–10555.
[136] S. Wu, X.-J. Kong, Y. Cen, J. Yuan, R.-Q. Yu, X. Chu, Fabrication of a lret-based upconverting hybrid nanocomposite for turn-on sensing of H2o2 and glucose, Nanoscale 8 (16) (2016) 8939–8946.
[137] D. Wang, K. Pan, Y. Qu, G. Wang, X. Yang, D. Wang, Bawo4:Ln3+ nanocrystals: controllable synthesis, theoretical investigation on the substitution site, and bright upconversion luminescence as a sensor for glucose detection, ACS Appl. Nano Mater. 1 (9) (2018) 4762–4770.
[138] H. Chen, A. Fang, L. He, Y. Zhang, S. Yao, Sensitive fluorescent detection of H2o2 and glucose in human serum based on inner filter effect of Squaric acid-iron(iii) on the fluorescence of upconversion Nanoparticle, Talanta 164 (2017) 580–587.
[139] Y. Liu, D. Tu, W. Zheng, L. Lu, W. You, S. Zhou, P. Huang, R. Li, X. Chen, A strategy for accurate detection of glucose in human serum and whole blood based on an upconversion Nanoparticles-polydopamine nanosystem, Nano Res. 11 (6) (2018) 3164–3174.
[140] J. Liu, L. Lu, A. Li, J. Tang, S. Wang, S. Xu, L. Wang, Simultaneous detection of hydrogen peroxide and glucose in human serum with upconversion luminescence, Biosensor. Bioelectron. 68 (2015) 204–209.
[141] T. Zhao, Y. Li, X. Zhang, H. Lyu, Z. Xie, A strategy for the accurate detection of glucose in human serum based on the ife effect of up-transformed Nanoparticles, Microchem. J. 186 (2023) 108363.
[142] H.D. Duong, J.I. Rhee, Use of cdse/zns Core-Shell quantum dots as energy transfer donors in sensing glucose, Talanta 73 (5) (2007) 899–905.
[143] Y. Gao, G. Wang, H. Huang, J. Hu, S.M. Shah, X. Su, Fluorometric method for the determination of hydrogen peroxide and glucose with Fe3o4 as catalyst, Talanta 85 (2) (2011) 1075–1080.
[144] E. Jang, S. Kim, W.-G. Koh, Microfluidic bioassay system based on Microarrays of hydrogel sensing elements entrapping quantum dot-enzyme conjugates, Biosensor. Bioelectron. 31 (1) (2012) 529–536.
[145] A. Fang, Q. Wu, Q. Lu, H. Chen, H. Li, M. Liu, Y. Zhang, S. Yao, Upconversion ratiometric fluorescence and colorimetric dual-readout assay for uric acid, Biosensor. Bioelectron. 86 (2016) 664–670.
[146] Y. Zhou, B. Ling, H. Chen, L. Wang, Mn2+-doped Nayf4:Yb, er upconversion Nanoparticles for detection of uric acid based on the Fenton reaction, Talanta 180 (2018) 120–126.
[147] Q. Wu, H. Chen, A. Fang, X. Wu, M. Liu, H. Li, Y. Zhang, S. Yao, Universal multifunctional nanoplatform based on Target-induced in situ promoting au seeds growth to quench fluorescence of upconversion Nanoparticles, ACS Sens. 2 (12) (2017) 1805–1813.
[148] L. Yang, X. Ren, X. Meng, H. Li, F. Tang, Optical analysis of lactate dehydrogenase and glucose by cdte quantum dots and their dual simultaneous detection, Biosensor. Bioelectron. 26 (8) (2011) 3488–3493.
[149] H. Chen, Q. Lu, K. He, M. Liu, Y. Zhang, S. Yao, A cyclic signal amplification strategy to fluorescence and colorimetric dual-readout assay for the detection of H2o2-related analytes and application to colorimetric logic gate, Sens. Actuator. B - Chem. 260 (2018) 908–917.
[150] H. Yuan, H. Zhao, K. Peng, F. Lv, L. Liu, J. Bao, S. Wang, Quantum dots for monitoring choline consumption process of living cells via an electrostatic force-mediated energy transfer, ACS Appl. Bio Mater. 2 (12) (2019) 5528–5534.
[151] R. Gill, L. Bahshi, R. Freeman, I. Willner, Optical detection of glucose and acetylcholine esterase inhibitors by H2o2-sensitive cdse/zns quantum dots, Angew. Chem. Int. Ed. 47 (9) (2008) 1676–1679.
[152] H. Chen, H. Zheng, W. Li, Q. Li, B. Hu, N. Pang, F. Tian, L. Jin, Ultrafast synthesized Monometallic nanohybrids as an efficient quencher and recognition antenna of upconversion Nanoparticles for the detection of xanthine with enhanced sensitivity and selectivity, Talanta 245 (2022) 123471.
[153] X. Liu, F. Wang, A. Niazov-Elkan, W. Guo, I. Willner, Probing biocatalytic transformations with luminescent DNA/Silver nanoclusters, Nano Lett. 13 (1) (2013) 309–314.
[154] J. Peng, A. Samanta, X. Zeng, S. Han, L. Wang, D. Su, D.T.B. Loong, N.-Y. Kang, S.-J. Park, A.H. All, W. Jiang, L. Yuan, X. Liu, Y.-T. Chang, Real-time in vivo hepatotoxicity monitoring through chromophore-conjugated photon-upconverting nanoprobes, Angew. Chem. Int. Ed. 56 (15) (2017) 4165–4169.
[155] X. Liu, H. Lai, J. Peng, D. Cheng, X.-B. Zhang, L. Yuan, Chromophore-modified highly selective ratiometric upconversion nanoprobes for detection of Onoo−-related hepatotoxicity in vivo, Small 15 (43) (2019) 1902737.
[156] X. Liu, L. He, X. Gong, Y. Yang, D. Cheng, J. Peng, L. Wang, X.-B. Zhang, L. Yuan, Engineering of reversible luminescent probes for real-time intravital imaging of liver injury and repair, CCS Chem. 4 (1) (2021) 356–368.
[157] Y. Zhong, J. Gu, Y. Su, L. Zhao, Y. Zhou, J. Peng, Real-time screening of hepatotoxins in natural medicine by peroxynitrite responsive lanthanide-based nir-ii luminescent probes, Chem. Eng. J. 433 (2022) 133263.
[158] Z. Sun, H. Huang, R. Zhang, X. Yang, H. Yang, C. Li, Y. Zhang, Q. Wang, Activatable Rare Earth near-Infrared-ii fluorescence ratiometric nanoprobes, Nano Lett. 21 (15) (2021) 6576–6583.
[159] C. Li, W. Li, H. Liu, Y. Zhang, G. Chen, Z. Li, Q. Wang, An activatable nir-ii nanoprobe for in vivo Early real-time diagnosis of traumatic brain injury, Angew. Chem. Int. Ed. 59 (1) (2020) 247–252.
[160] X. Yang, Z. Wang, H. Huang, S. Ling, R. Zhang, Y. Zhang, G. Chen, C. Li, Q. Wang, A Targeted activatable nir-iib nanoprobe for highly sensitive detection of ischemic stroke in a photothrombotic stroke model, Adv. Healthcare Mater. 10 (5) (2021) 2001544.
[161] X. Yang, X. An, S. Ling, H. Huang, Y. Zhang, G. Chen, C. Li, Q. Wang, A Cascade Targeted and activatable nir-ii nanoprobe for highly sensitive detection of acute myeloid leukemia in an orthotopic model, CCS Chem. 3 (3) (2020) 895–903.
[162] H. Huang, Z. Sun, H. Yang, X. Yang, F. Wu, Y. Sun, C. Li, M. Tian, H. Zhang, Q. Wang, Precise examination of peripheral Vascular disease for diabetics with a novel multiplexed nir-ii fluorescence imaging technology, Nano Today 43 (2022) 101378.
[163] Z. Li, L. Xiao, Facile sonochemical synthesis of water-soluble gold nanodots as fluorescent probes for superoxide radical anion detection and cell imaging, Anal. Methods 9 (12) (2017) 1920–1927.
[164] Y. Yan, J. Sun, K. Zhang, H. Zhu, H. Yu, M. Sun, D. Huang, S. Wang, Visualizing gaseous nitrogen dioxide by ratiometric fluorescence of Carbon nanodots-quantum dots hybrid, Anal. Chem. 87 (4) (2015) 2087–2093.
[165] L. Zhao, J. Peng, M. Chen, Y. Liu, L. Yao, W. Feng, F. Li, Yolk-Shell upconversion nanocomposites for lret sensing of cysteine/homocysteine, ACS Appl. Mater. Interfaces 6 (14) (2014) 11190–11197.
[166] J. Ni, C. Shan, B. Li, L. Zhang, H. Ma, Y. Luo, H. Song, Assembling of a functional cyclodextrin-decorated upconversion luminescence nanoplatform for cysteine-sensing, Chem. Commun. 51 (74) (2015) 14054–14056.
[167] Y. Guan, S. Qu, B. Li, L. Zhang, H. Ma, L. Zhang, Ratiometric fluorescent nanosensors for selective detecting cysteine with upconversion luminescence, Biosensor. Bioelectron. 77 (2016) 124–130.
[168] K. Wang, J. Qian, D. Jiang, Z. Yang, X. Du, K. Wang, Onsite naked eye determination of cysteine and homocysteine using quencher displacement-induced fluorescence recovery of the dual-emission hybrid probes with desired intensity ratio, Biosensor. Bioelectron. 65 (2015) 83–90.
[169] L. Shang, S. Dong, Sensitive detection of cysteine based on fluorescent silver clusters, Biosensor. Bioelectron. 24 (6) (2009) 1569–1573.
[170] R. Deng, X. Xie, M. Vendrell, Y.-T. Chang, X. Liu, Intracellular glutathione detection using Mno2-nanosheet-modified upconversion Nanoparticles, J. Am. Chem. Soc. 133 (50) (2011) 20168–20171.
[171] Y. Wang, Y. Li, Z. Zhang, L. Wang, D. Wang, B.Z. Tang, Triple-jump photodynamic theranostics: Mno2 combined upconversion nanoplatforms involving a type-I photosensitizer with aggregation-induced emission Characteristics for potent cancer treatment, Adv. Mater. 33 (41) (2021) 2103748.
[172] H. Zhao, Y. Li, X. Zhang, K. Wu, J. Lv, C. Chen, H. Liu, Z. Shi, H. Ju, Y. Liu, Orthogonal excitations of lanthanide Nanoparticle up/down conversion emissions via switching nir lights for in-vivo theranostics, Biomaterials 291 (2022) 121873.
[173] S. Wang, Z. Wei, L. Li, X. Ning, Y. Liu, Luminescence imaging-guided triple-collaboratively enhanced photodynamic therapy by bioresponsive lanthanide-based nanomedicine, Nanomed.-Nanotechnol. Biol. Med. 29 (2020) 102265.
[174] Y. Li, H. Zhang, C. Guo, G. Hu, L. Wang, Multiresponsive nanoprobes for turn-on Fluorescence/(19)F mri dual-modal imaging, Anal Chem 92 (17) (2020) 11739–11746.
[175] Y. Zhang, Q. Ma, Y. Yan, C. Guo, S. Xu, L. Wang, Intratumoral glutathione activatable nanoprobes for fluorescence and (19)F magnetic resonance turn-on imaging, Anal Chem 92 (23) (2020) 15679–15684.
[176] D. Song, M. Zhu, C. Li, Y. Zhou, Y. Xie, Z. Li, Z. Liu, Boosting and activating nir-iib luminescence of Ag(2)Te quantum dots with a Molecular trigger, Anal Chem 93 (50) (2021) 16932–16939.
[177] X. Zhang, F.-G. Wu, P. Liu, N. Gu, Z. Chen, Enhanced fluorescence of gold nanoclusters composed of Haucl4 and histidine by glutathione: glutathione detection and selective cancer cell imaging, Small 10 (24) (2014) 5170–5177.
[178] T.H. Chen, W.L. Tseng, (Lysozyme type vi)-stabilized Au8 clusters: synthesis mechanism and application for sensing of glutathione in a single drop of blood, Small 8 (12) (2012) 1912–1919.
[179] Y. Yang, Y. Yu, H. Chen, X. Meng, W. Ma, M. Yu, Z. Li, C. Li, H. Liu, X. Zhang, H. Xiao, Z. Yu, Illuminating platinum transportation while maximizing therapeutic efficacy by gold nanoclusters via simultaneous near-Infrared-I/Ii imaging and glutathione scavenging, ACS Nano 14 (10) (2020) 13536–13547.
[180] T. Liang, Z. Li, P. Wang, F. Zhao, J. Liu, Z. Liu, Breaking through the signal-to-background limit of upconversion nanoprobes using a Target-modulated sensitizing switch, J. Am. Chem. Soc. 140 (44) (2018) 14696–14703.
[181] J. Xu, Y. Kuang, R. Lv, P. Yang, C. Li, H. Bi, B. Liu, D. Yang, Y. Dai, S. Gai, F. He, B. Xing, J. Lin, Charge convertibility and near Infrared photon co-enhanced cisplatin chemotherapy based on upconversion nanoplatform, Biomaterials 130 (2017) 42–55.
[182] M. Zhao, H. Zhuang, H. Zhang, B. Li, J. Ming, X. Chen, M. Chen, A lret nanoplatform consisting of lanthanide and amorphous manganese oxide for nir-ii

luminescence lifetime imaging of tumor redox status, Angew. Chem. Int. Ed. 61 (47) (2022) e202209592.
[183] Y. Liu, X. Zhu, Z. Wei, W. Feng, L. Li, L. Ma, F. Li, J. Zhou, Customized photothermal therapy of subcutaneous orthotopic cancer by multichannel luminescent nanocomposites, Adv. Mater. 33 (30) (2021) e2008615.
[184] Y. Liu, X. Zhu, Z. Wei, K. Wu, J. Zhang, F.G. Mutti, H. Zhang, F.F. Loeffler, J. Zhou, Multi-Channel lanthanide nanocomposites for customized synergistic treatment of orthotopic multi-tumor cases, Angew. Chem. Int. Ed. 62 (30) (2023) e202303570.
[185] Y. Zhang, Y. Li, X.-P. Yan, Photoactivated cdte/cdse quantum dots as a near Infrared fluorescent probe for detecting biothiols in biological fluids, Anal. Chem. 81 (12) (2009) 5001–5007.
[186] B. Han, J. Yuan, E. Wang, Sensitive and selective sensor for biothiols in the cell based on the recovered fluorescence of the cdte quantum Dots−Hg(Ii) system, Anal. Chem. 81 (13) (2009) 5569–5573.
[187] N. Zhang, F. Qu, H.Q. Luo, N.B. Li, Sensitive and selective detection of biothiols based on Target-induced Agglomeration of silvernanoclusters, Biosensor. Bioelectron. 42 (2013) 214–218.
[188] L. Zhang, Q.-Y. Cai, J. Li, J. Ge, J.-Y. Wang, Z.-Z. Dong, Z.-H. Li, A label-free method for detecting biothiols based on poly(thymine)-templated copper Nanoparticles, Biosensor. Bioelectron. 69 (2015) 77–82.
[189] W. Di, N. Shirahata, H. Zeng, Y. Sakka, Fluorescent sensing of colloidal Cepo4: tb nanorods for rapid, ultrasensitive and selective detection of vitamin C, Nanotechnology 21 (36) (2010) 365501.
[190] Y.-J. Chen, X.-P. Yan, Chemical redox modulation of the Surface chemistry of cdte quantum dots for probing ascorbic acid in biological fluids, Small 5 (17) (2009) 2012–2018.
[191] Y. Cen, J. Tang, X.-J. Kong, S. Wu, J. Yuan, R.-Q. Yu, X. Chu, A cobalt oxyhydroxide-modified upconversion nanosystem for sensitive fluorescence sensing of ascorbic acid in human plasma, Nanoscale 7 (33) (2015) 13951–13957.
[192] J.S. Anjali Devi, S. Salini, A.H. Anulekshmi, G.L. Praveen, G. Sony, Fe (iii) ion modulated L-dopa protected gold nanocluster probe for fluorescence turn on sensing of ascorbic acid, Sensor. Actuat. B - Chem. 246 (2017) 943–951.
[193] A. Wu, H. Ding, W. Zhang, H. Rao, L. Wang, Y. Chen, C. Lu, X. Wang, A colorimetric and fluorescence turn-on probe for the detection of ascorbic acid in living cells and beverages, Food Chem. 363 (2021) 130325.
[194] X.-B. Zhang, Z.-Q. Liang, X. Yan, M.-M. Li, C.-Q. Ye, X.-M. Wang, X.-T. Tao, The effect of triethylamine on dye-sensitized upconversion luminescence and its application in nanoprobes and photostability, Phys. Chem. Chem. Phys. 25 (17) (2023) 12401–12408.
[195] P. Zhao, K. He, Y. Han, Z. Zhang, M. Yu, H. Wang, Y. Huang, Z. Nie, S. Yao, Near-Infrared dual-emission quantum dots-gold nanoclusters nanohybrid via co-template synthesis for ratiometric fluorescent detection and bioimaging of ascorbic acid in vitro and in vivo, Anal. Chem. 87 (19) (2015) 9998–10005.
[196] Z. Jie, G. Qi, C. Xu, Y. Jin, Enzymatic Preparation of plasmonic-fluorescent quantum dot-gold hybrid nanoprobes for sensitive detection of glucose and alkaline phosphatase and dual-modality cell imaging, Anal. Chem. 91 (21) (2019) 14074–14079.
[197] R. Freeman, R. Gill, I. Shweky, M. Kotler, U. Banin, I. Willner, Biosensing and probing of Intracellular metabolic pathways by nadh-sensitive quantum dots, Angew. Chem. Int. Ed. 48 (2) (2009) 309–313.
[198] P. Harvey, C. Oakland, M.D. Driscoll, S. Hay, L.S. Natrajan, Ratiometric detection of enzyme turnover and flavin reduction using Rare-Earth upconverting phosphors, Dalton Trans. 43 (14) (2014) 5265–5268.
[199] L. Burgess, H. Wilson, A.R. Jones, P. Harvey, L.S. Natrajan, S. Hay, Covalent attachment of active enzymes to upconversion phosphors allows ratiometric detection of substrates, Chem.-A Eur. J. 26 (65) (2020) 14817–14822.
[200] S. Li, Z. Wang, S. Chen, J. Gu, Y. Ma, J. Jiang, R. Zhang, D. Zhang, Y. Wang, H. Wang, Ratiometric fluorescence sensing based on Rare-Earth upconversion Nanoparticles for the rapid identification of antioxidant capacity, New J. Chem. 47 (4) (2023) 2079–2085.